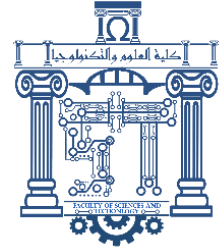*Republique Algerienne Democratique Et Populaire*
Ministère de l'Enseignement Supérieur et de la Recherche Scientifique
Université Chahid Chikh Larbi Tébessi – Tébessa –
Faculté des Sciences et de la Technologie
Département de Genie Mecanique

Mémoire de fin d'étude
Pour l'obtention du diplôme de Master
Option : énergétique
Thème

Application des nanofluides dans le transport de l'énergie thermique

Nanofluids applications in thermal energy transport

Encadré par :   Présenté par :

Pr. BELAZIZIA Abdennacer   **OUAHICH Chaima, BOUMAAGOUDA Chaima**

Présenté et soutenu publiquement, le   07 / 06 / 2023   , devant le jury composé de :

Dr. BOUAFFANE Abdelkrim	**Université de Tébessa**	**Président**
Pr. BELAZIZIA Abdennacer	**Université de Tébessa**	**Rapporteur**
MCA. CHELLOUG F. Zohra	**Université de Tébessa**	**Examinateur**

Promotion : 2022-2023

شكر وتقدير

بادئ ذي بدء نشكر الله العلي القدير، القوي المتين

على توفيقه لنا في انجاز هذا البحث و نحمده حمدًا كما ينبغي لجمال

وجهه و عظيم سلطانه مصداقًا لقوله

عزّوجل: ''وَ اُشْكُرُوا لِي وَ لَا تَكْفُرُونَ ''[الآية 152من سورة البقرة]

والشكر موصول لأستاذنا الفاضل الدكتور**" بلعزيزية عبد الناصر"**

الذي منحنا من جهده ووقته الكثير، في الاشراف و التوجيه و قراءة الموضوع كما

نتقدم بالشكر والعرفان الى كل من ساعدنا من قريب او من بعيد و كانوا

مرشدين وموجهين لنا دائمًا.

إهْدَاء

إلى خالدة الذكر، التي وافتها المنيَّة منذ سنة، وكانت خير مثال لربة الأسرة، والتي لم تتهاون يوم في توفير سبيل الخير والسعادة لي، " أُمي الحبيبة."

الى من تحمل المشقة وتعِب ليُوفر لي كل الامكانيات في مسيرتي الدراسية،"والدي الفاضل"

إلى من أعتمد عليهما في كل صغيرة وكبيرة،" أخويَّ المُحترمان"

الى من اتمنى لها التوفيق والنجاح في كل سُبُل حياتها،"اختي العزيزة"

إلى أصدقائي ومعارفي الذين أُجلُّهم وأحترمُهم... إلى أساتذتي في الكلية...

الى كل من علمني حرفا في هذه الدنيا الفانية...

أُهديكم عملي المتواضع.

وحيش شيماء

إهْدَاء

الحمد لله حمدا كثيرا طيبا مباركا فيه والصلاة والسلام على خير المرسلين حبيبنا المصطفى خير من نطق بالهدى والصواب اما بعد:

الحمد لله الذي احلنا محلة الفهم وحلانا حلية العلم، وملكنا عقال العقل وزيننا بنطق المنطق، الحمد لله الذي بلغنا مبلغنا هذا ورزقنا خير الرزق هذا من غير حول منا ولا قوة، ووفقنا فيه أحسن التوفيق سبحانه وتعالى.

لسندي وقرة عيني، لنبضي ومن اعزها في قلبي، لقدوتي وملهمي، لمن حثني على الدراسة وساندني فيها، ادامهم الله تاجا على رأسي.

لإخوتي واختي حفضهم الله ورعاهم، الى استاذتي الكرام إلى كل من علمني حرفا او اعانني على تعلمه، الى كل قسم الهندسة الميكانيكية وكل دفعة 2023م
جامعة الشيخ الشهيد العربي التبسي، تبسة.

الى كل من احبه قلبي ونسيه قلمي وكل من كان له أثر طيب في حياتي.

بو معقودة شيماء

List of contents

Chapter I: Generalities of nanofluids

Chapter II : Geometry and mathematic modeling

Chapter III: numerical and mathematic formulation

chapter IV: Results and descent

Abstract

Natural convection in inclined square enclosure filled with a nano fluid is studied numerically using finite volume method. Our results were based on the effect of: Rayleigh number$500 \leq Ra \leq 10^6$, volume fraction of nano particles$0 \leq \varphi \leq 0.2$, anclinaision angle$0° \leq \alpha \leq 90°$, and the type of nanoparticules (Cu, Al2o3, and Au) on heat transfer, fluid structure and velocity flow in the enclosure. The obtained results show that heat transfer rate increases with the increase of Ra or φ. Heat transfer is greater with Cu-water nano fluid and it reaches the maximum value when the inclination angle α =30°.

Keywords: Natural convection, Nano fluid, inclination angle, Laminar flow, Cartesian geometry, Volume method.

Résumé

La convection naturelle dans une cavité carrée inclinée remplit par un nano fluide est étudiée numériquement par la méthode des volumes finies. Nos résultants ont été basées sur l'influence des paramètres: nombre de Rayleigh$500 \leq Ra \leq 10^6$, la fraction volumique des nanoparticules$0 \leq \varphi \leq 0.2$, l'angle d'inclinaison $0° \leq \alpha \leq 90°$ et le type des nanoparticules (Cu, Al2o3, Au) sur le transfert de chaleur, la structure d'écoulement et la vitesse de l'écoulement dans l'enceinte. Les résultats obtenus montrent que le taux du transfert de chaleur augmente avec les nombres Ra et φ. Le transfert de chaleur et meilleur avec le nano fluide à base d'eau formé par les nano particules métallique (Cu). Il atteint son maximum avec l'angle d'inclinaison α =30°.

Mots clés: Convection naturelle, nano fluide, angle d'inclinaison, écoulement laminaire, géométrie cartésienne, Volume finie.

الملخص

قمنا بدراسة عددية باستعمال طريقة الحجوم المنتهية للحمل الطبيعي داخل تجويف مربع الشكل مائل و مملوء بمائع نانوي. تتمحور الدراسة حول ابراز اثر الاعداد: رايلي $10^6 \geq Ra \geq 500$, النسبة الحجمية للجسيمات النانوية $0.2 \geq \varphi \geq 0$, زاوية الميلان $90° \geq \alpha \geq 0°$ و نوع الجسيمات النانوية (Al2o3, Au,Cu) على نسبة انتقال الحرارة وكذا شكل وسرعة الجريان. النتائج المتحصل عليها تبين ان نسبة انتقال الحرارة تزداد مع زيادة الاعداد Ra و φ . انتقال الحرارة يكون اكبر في حالة الموائع النانوية المشكلة من الجزيئات المعدنية و يكون اعضميا في حالة زاوية الميلان تساوي °30.

الكلمات المفتاحية: الحمل الحراري الطبيعي , المائع النانوي , زاوية الميلان , النظام المستقر , الشكل الهندسي الكارتيزي, طريقة الحجوم المنتهية.

List of figures

List of tables

Nomenclature

Latin letters

Cp	Specific heat	$(J.kg^{-1}.K^{-1})$
g	Gravitational acceleration	$(m.s^{-2})$
H	cavity length	(m)
λ	Thermal conductivity	$(W.m^{-1}.K^{-1})$
Nu	Nusselt number	
P	Dimensionless pressure	
Pr	Prandtl number	
Ra	Rayleigh number	
T	Absolute temperature	(K)
T_h	Hot temperature	(K)
T_c	Cold temperature	(K)
t	Time	(S)
U, V	Dimensionless velocity components	
u,v	Velocity component in x and y directions	$(m.s^{-1})$
x,y	Coordinate system	
X,Y	Dimensionless coordinates	

Greeks symbols

α_{nf}	Thermal diffusivity of nanofluid	$(m^2.s^{-1})$
β	Thermal expansion coefficient	(K^{-1})
α	Inclination angle of the cavity	°
ϑ	Cinematic viscosity	$(m^2.s^{-1})$
μ	Dynamic viscosity	$(N.s.m^{-2})$
ΔT	The temperature difference	
φ	Nanoparticles volume fraction	
ρ	Density	$(Kg.m^{-3})$
τ	Dimensionless time	
θ	Dimensionless temperature	

Subscripts

f	Base fluid
nf	Nano-fluides
p	Nanoparticle
max	Maximal
min	minimal

GENERAL INTRODUCTION

INTRODUCTION

Thermal transfer is embodied as a process of transferring thermal energy from one object or system to another, as its importance has emerged in engineering and technology for the design and operation of various systems such as cooling and heating systems in buildings, vehicles and electronic devices.

Nanofluids are liquid materials that contain nanoparticles that can improve the thermal properties of liquids, increase heat transfer efficiency, and reduce energy consumption, which distinguishes nanofluids from other fluids.

The idea is introducing nanoparticles into the base fluid in order to increase the thermal conductivity of the mixture. Therefore, this improvement in heat transfer makes nanofluids a promising new technology in the context of heat transfer, which makes it possible to improve the performance of various heat exchangers.

Heat transfer by convection is the main objective of many works. A large number of researchers conducted a large number of numerical and experimental tests related to the description of the phenomena that govern convection and the impact of the nature of the systems in which it occurs (especially engineering).

In this study we will be particularly interested in studying heat transmission in a square cavity, filled with a nanofluid, and subjected to horizontal temperature gradient. Finite volume method is used to solve the governing equations. The effect of Rayleigh number, volume fraction of nano particles in the base fluid, and the inclination angle on convection heat transfer in the enclosure is studied. The effect of the type of nano particles is also considered.

Our study is divided to four chapters: generality about nanofluids, geometry and mathematic formulation, numerical method, results and discussions, and finally a conclusion.

CHAPTER I
GENERALITIES
OF NANOFLUIDS

I.1 Introduction

Nano fluids are a new generation of mixtures, while many studies have been carried out to better understand their properties, further studies are still needed. A brief overview of the developments on the subject has been collected in this part. It does not cover all field work, but it shows the complexity of the problem of the properties of nanofluids and the wide range of efforts which have been dedicated to solving it [1].

Nanofluids are colloidal solutions made up of particles of nanometric size suspended in a carrier liquid. This type of solution has aroused great interest since the discovery of their particular thermal properties. Indeed, base fluids often used in cooling or heating applications have conductivities very low thermals which limit their ability to transfer heat. The idea then is to insert very high conductivity nanoparticles into the base liquids, in order to increase the effective thermal conductivity of the mixture and thus improve its thermal performance.

The choice of base liquids is essential for nanofluids, it ensures the stability of the suspension in time and to avoid any phenomenon of aggregations, the selection of such a fluid will be ironed depending on the nature of the nanoparticle, the most used solvents are:

• The water.

• Ethylene glycol, EG.

• The oils.

• Toluene.

• Refrigeration fluids.

I.2 Nanoparticles and carrier fluid

Nanoparticles are particles whose 3 dimensions are in the range 1-100 nm approximately. Nanomaterials are objects in which at least one of their three dimensions is nanometric, i.e. less than 100 nm. However, this definition is still in Discussion and some definitions speak of nanoparticles as soon as one or two of their dimensions is less than 100nm.

The basic liquids generally used in the preparation of nanofluids are those used common in heat transfer applications such as water, ethylene glycol, oil...Finally the nanoparticles can be based on metals, oxides, carbides, nitrides or carbon [2].

I.2.1 Nanoparticle size

The manufacturing processes are of a physical or chemical nature. They are the subject of much of research to improve the cost of production which remains sometimes high considering the difficulties of implementation and to obtain particles of the desired size. Various chemical and physical techniques are physical techniques are available to elaborate nanoparticles. These different methods make it possible to obtain free or coated nanoparticles, encapsulated in a host matrix. If the idea of using solid particles in suspension to improve heat exchange is old, since it stems exchange is old, since it stems in particular from Maxwell's

Analytical studies around 1873 [3], it is only since the 1990's that the use of nanoscale particles has been studied. Nanometer scale particles have been studied. This has been made possible by the development of particular and innovative manufacturing processes.
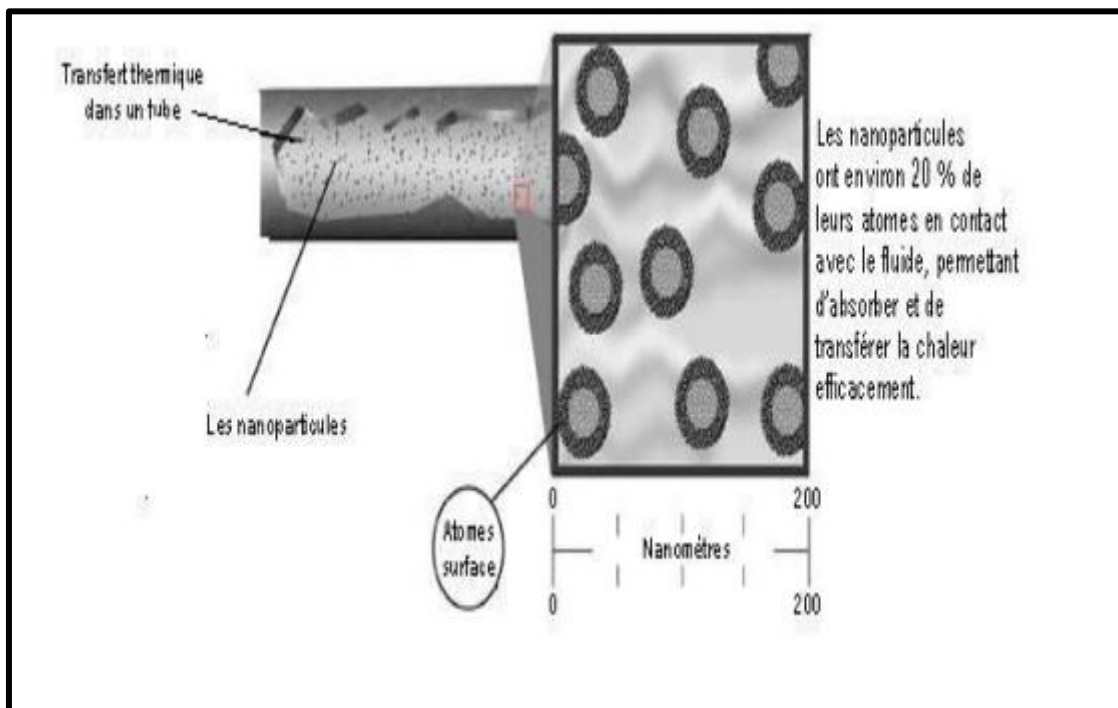
Figure (I.1): Nanoparticles in a pipe.

I.2.2 The physical terms of nanoparticles

➕ Metallic nanoparticles :

To: $T = 20°C$ and P =1 atm

Table (I. 1): The physical terms of metallic nanoparticles.

nanoparticle	Tailed (nm)	Density $\rho\ (kg.m^{-3})$	heat capacity $Cp\ (J.kg^{-1}.k^{-1})$	thermal conductivity $\lambda\ (w.m^{-1}.k^{-1})$
aluminum	20-26	2719	871	202.4
Copper	60-80	8960	380	401
gold (Au)	10	19300	150	320
silver (Ag)	18	10500	235	429
Silicone (Si)	19	2329	280	148
iron (Fe)	20	7870	447	80.2
Nickel	20	8900	444	90.7
Sic	40	3160	775	490
Pt	15	21450	133	71.6
Ir	10-25	22500	130	147

➕ Nonmetallic nanoparticles

To: $T = 20°C$ and P=1 atm

Table (I. 2): The physical terms of non-metallic nanoparticles.

non-metallic nanoparticles	Density $\rho\ (kg.m^{-3})$	heat capacity $Cp\ (J.kg^{-1}.k^{-1})$	thermal conductivity $\lambda\ (w.m^{-1}.k^{-1})$
CNT	depending on the number of fibers	depending on the number of fibers	2500
Diamante (C)	3500	509	2300

✚ Oxide nanoparticles:

To: $T = 20°C$ and P=1 atm

Table (I.3): The physical terms of oxide nanoparticles.

nanoparticles	Tailed (nm)	Density $\rho \ (kg.m^{-3})$	heat capacity $Cp \ (J.kg^{-1}.k^{-1})$	thermal conductivity $\lambda \ (w.m^{-1}.k^{-1})$
AL2O3	20-50	3970	765	50
SiO2	20	2650	745	13.4
CuO	40	6315	350	76.5
CO	20	8865	421	99.2
TiO2	10-30	4157	710	7.9

✚ Base fluid

To: = 20°C , P=1 atm

Table (I.4): The physical terms of based fluid.

Fluid	Density $\rho \ (kg.m^{-3})$	heat capacity $Cp \ (J.kg^{-1}.k^{-1})$	thermal conductivity $\lambda \ (w.m^{-1}.k^{-1})$	dynamic viscosity $\mu \ (Pa.s)$
water	1000.1	4182	0.613	10.1×10^{-4}
Ethylene glycol, EG.	1132	2349	0.258	16×10^{-3}
R12 (liquid)	1194.9	0.965	70.95*10	22.5×10^{-5}
R134a (liquid)	1196.2	1.41	84.4*10	214×10^{-6}

> **thermo-physical properties of Nano fluid (water+CuO) for different concentrations**

To: $T = 20°C$ and P= 1 atm

Table (I.5): Thermo-physical properties of Nano fluid (water+CuO).

Mass Ratio	CuO (g)	Thermal Conductivity (W/mK)	Melting Temperature (°C)
0	0	0.25	64.22
0.05	0.0974	0.53	63.62
0.10	0.1950	1.55	63.59
0.15	0.2920	1.91	63.66
0.20	0.3900	1.97	63.19
0.25	0.4890	2.07	62.45

I.2.3 Different types of nanoparticles

The production of new nanomaterials (nanoparticles) is a rapidly growing field of research. Field, so only the most commonly used nanoparticles in heat transfer applications are briefly mentioned here. Applications are briefly mentioned here [3].

Generally speaking, nanoparticles can be classified according to their form into two main categories:

1. Spherical nanoparticles for which several types of materials can be used for their fabrication for their manufacture. These spherical nanoparticles can be based on metals (copper Cu, iron Fe, gold Au, silver Ag...) or copper oxides (aluminum oxide Al2O3, copper oxide CuO, titanium oxide TiO2...).

2. Nanopipes (Carbone nanotubes CNT, titanium Nanopipes TiO2, silicone Nanopipes...).

I.3 Methods of preparing Nanofluids

Nano fluids are produced by several techniques: first step, second step, and other techniques. To avoid the sedimentation of nanoparticles during its operation, surfactant may be added to them. Nano fluid preparation is the first step ahead of any implementations. Therefore, it entails more focus from researchers to obtain a good stage of stability. Colloidal theory states that sedimentation in suspensions ceases when the particle size is below a critical radius due to counterbalancing gravity forces by the Brownian forces.

Nanoparticles of a smaller size may be a better size in the different applications. However, it has a high surface which leads to the formation of agglomerates among them. Therefore, to obtain a stable Nano fluid with optimum particle diameter and concentration, it is considered a big challenge for researchers. Two common methods are used to produce Nano fluids, the two-step method and the one step method, and others have worked up some innovations [4].

I.3.1 The two-step method

The two-step method is the common method to produce nanofluids. Nanoparticles of different materials including Nano fibers, nanotubes, or other Nanomaterials are first produced as Nano sized from 10 to 100 nm by chemical or physical methods. Then, the Nano-sized powder will be dispersed in base fluids with the help of intensive magnetic force agitation, ultrasonic agitation, high-shear mixing, homogenizing, and ball milling. As resulting from high surface area and surface activity, nanoparticles tend to aggregate reflecting adversely on the stability of nanofluids. To avoid that effect, the surfactant is added to the nanofluids [4].
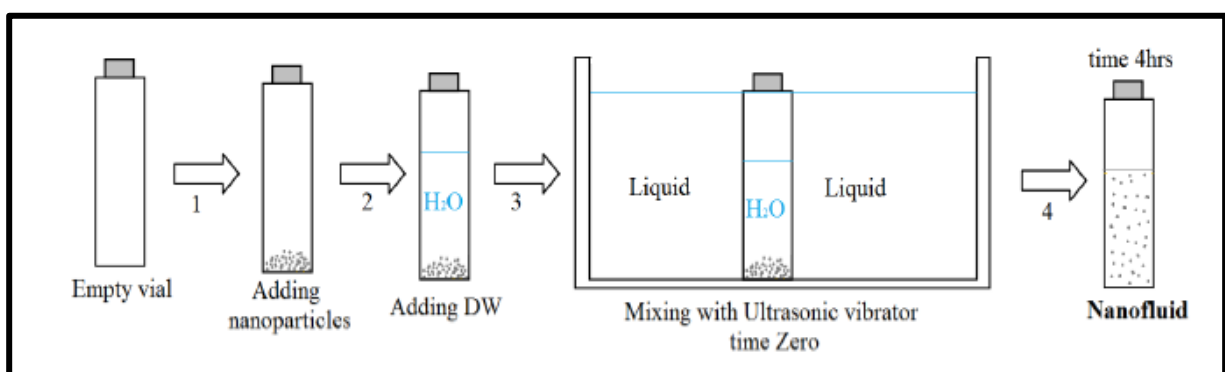
Figure (I.2): Block diagram of preparation of two-step method [5].

I.3.2 One-step method

The one-step process is simultaneously making and dispersing the particles in the base fluids which could be reduced to the agglomeration of nanoparticles. This method makes the nanofluids more stable with a limitation of the high cost of the process.
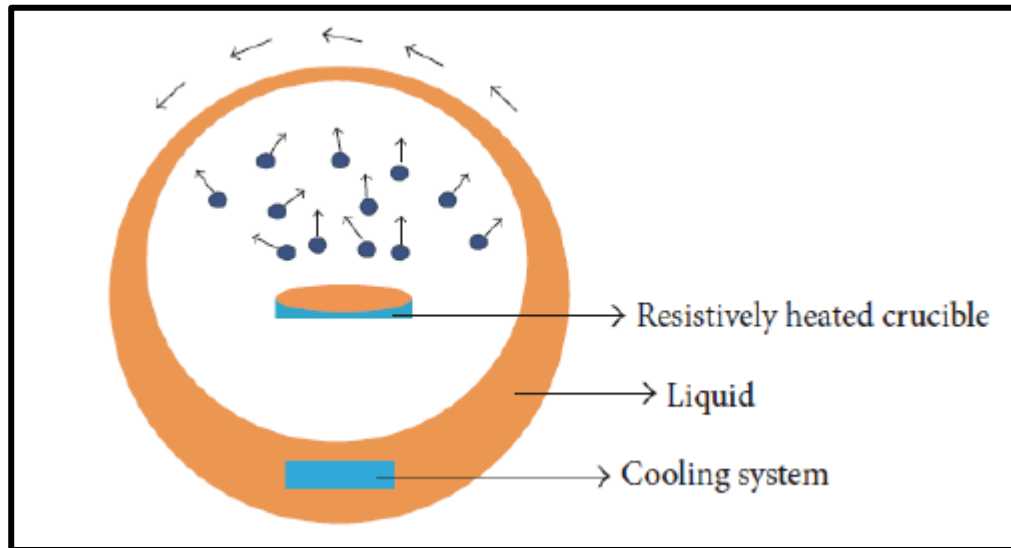
Figure (I.3): One-step process presentation [5].

I.4 Thermo physical properties of Nano fluids

Nano fluids have novel properties different from base fluids that included thermo physical properties such as specific heat, density, viscosity, and thermal conductivity. Mixing the nanoparticles into a base fluid changes its thermo physical properties. The most important thermo physical properties of Nano fluids are Nano fluid viscosity, Nano fluid convective heat transfer, Nano fluid thermal conductivity, and Nano fluid specific heat.

The value of specific heat and density of the Nano fluids can be determined by correlations, whereas the viscosity and thermal conductivity have different correlations [4].
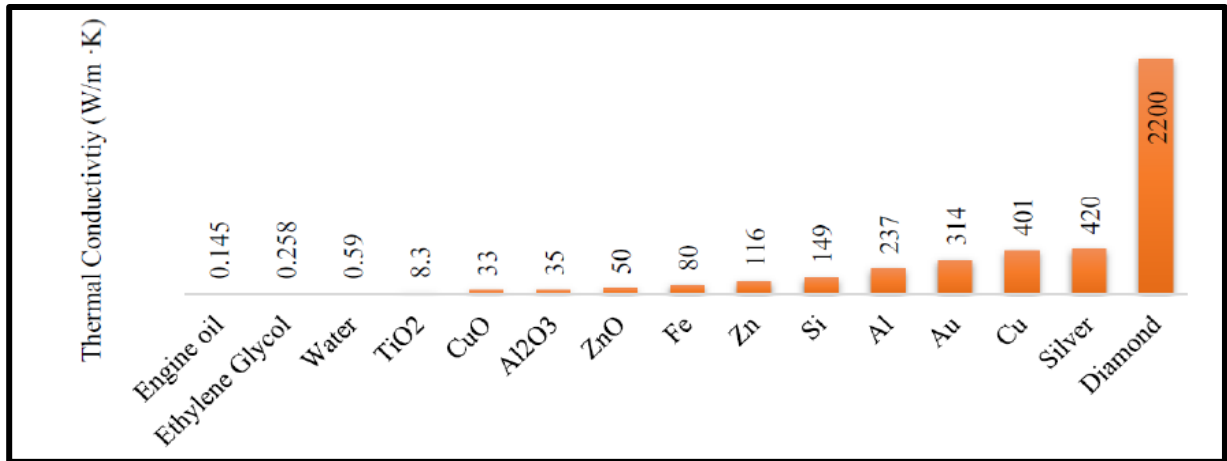
Figure (I.4): The thermal conductivity of different base fluids and
Solids materials at 298, 15 K [5].

I.4.1 The volume fraction (φ)

The volume fraction is the most important property for the nano-fluid, since the calculations of all the other properties are based on the volume fraction of the nano-fluid. Nonetheless, we can define the volume fraction as the volume of solid or particle (nano-particles) over the total volume (nano-particles + base fluid). The value of the volume fraction is varied between 0 (pure base fluid) and 1. The volume fraction is given by the following relation:

$$\varphi = \frac{v_p}{v_T} \qquad\qquad\qquad \textbf{(I.1)}$$

v_p: Volume of solid (Nano-particles).

v_T: Total volume.

The physical-thermodynamic properties of nano-fluids depend mainly on the quality of the base fluid and the quality of the dissolved nano-particles in the basic liquid. Among the parameters that control the determination of the properties of the nano-particle: thermal conductivity, dynamic and kinematic viscosity, specific heat capacity, etc. In addition to that the shape, diameter of Nano-particles, the concentration of suspended particles and the temperature of the Nano-fluids also influence the physical properties of the Nano-fluids [5].
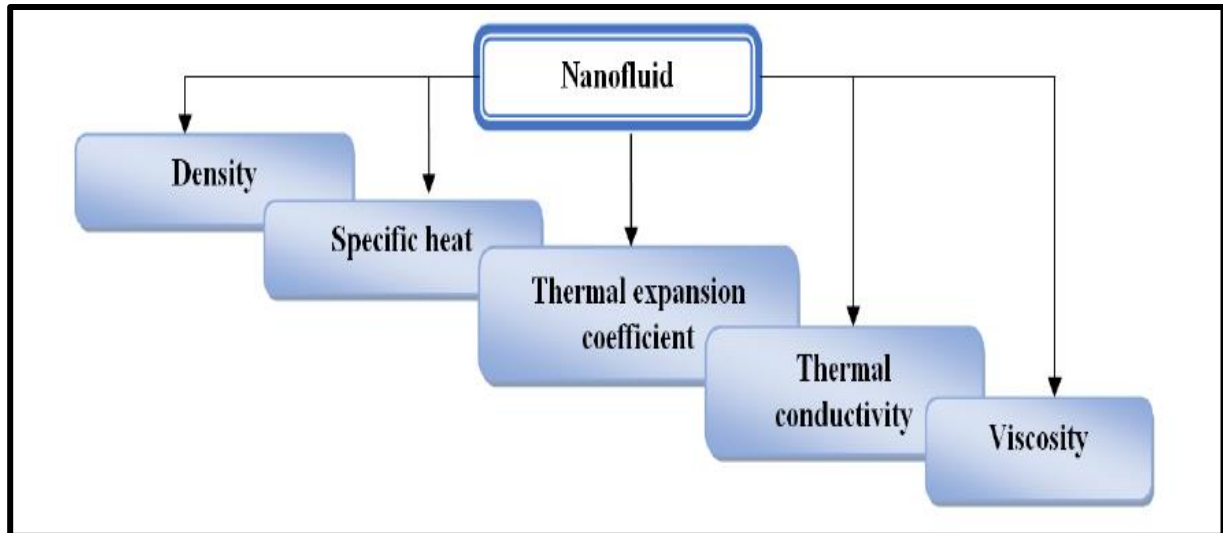
Figure (I.5): thermophysical properties of Nano fluids**.**

I.4.2 The density

The density of a perfectly homogeneous Nano-fluid is determined (good dispersion of the Nano-particles in the fluid) as a function of the volume fraction φ at a given temperature T, is made from the definition of the density of a mixture [5].

We then reduce the density of the Nano-fluid:

$$\rho_{nf} = (1 - \varphi)\rho_{bf} + \varphi\rho_p \qquad \qquad \text{(I.2)}$$

I.4.3 Specific heat

Specific heat is one of the essential properties and has an essential role in influencing the thermal transfer rate of Nano fluids. Specific heat is the quantity of heat needed to raise the temperature of one gram of Nano fluid by one degree centigrade .Sang and Liu conducted studies with four different nanoparticles (SiO2, CuO, TiO2 and Al2O3) to investigate the specific increase in heat capacity of ternary carbonate. Their experimental data asserts that the SiO2 nanoparticle is the best particle to improve the specific heat capacity of ternary carbonate Nano fluids, and they showed that the specific heat capacity of the Nano fluid depends mainly on the type of nanoparticle and the nanostructure. Sardinia et al. experimented with the specific thermal capacities of CuO-based oil Nano fluids with particle weight fractions of 0.2–2% at different temperatures. In this experiment, the Nano fluids showed a less specific heat capacity than the base fluid, and it decreased with the increasing concentration of the Nano fluids. This result indicates that the specific heat of Nano fluids at a fraction of 2% by weight is about 23% lower than that of the base fluid at 40 °C. The specific heat of a Nano fluid is determined by two formulas.

➕ Or the first is estimated by Pak and Cho (1998) as follows:

$$\left(C_p\right)_{nf} = (1 - \varphi)(Cp)_{bf} + \varphi(Cp)_p \qquad \text{(I.3)}$$

➕ Or the second is estimated by Xuan and Roetzel (2000) as follows:

$$\left(\rho C_p\right)_{nf} = (1 - \varphi)(\rho Cp)_{bf} + \varphi(\rho Cp)_p \qquad \text{(I.4)}$$

I. 4. 4. The thermal expansion coefficient

In the context of our study, we are only interested in incompressible fluids (density independent of pressure). This variation in density under the action of temperature is characterized by the coefficient of thermal expansion, also called the coefficient of expansion(Bejan,)
To calculate the value of this coefficient for Nano-fluids, we use this expression:

$$\rho_{nf}\beta_{nf} = (1 - \varphi)\rho_f\beta_f + \varphi\rho_s\beta_s \qquad \text{(I.5)}$$

Kim et al. assumed that the coefficient of thermal expansion of the fluid $(\beta_s)$is much greater than that of solid Nano-particles(β_s). They reduced equation to the following simplified form[5]

$$\rho_{nf}\beta_{nf} = (1 - \varphi)\rho_f\beta_f \qquad \text{(I.6)}$$

I.4.5 Thermal conductivity

The thermal conductivity, noted λ $(W.m^{-1}.K^{-1})$, is the ability of a material to conduct or transmit heat, the thermal conductivity is improved by several tens of percent compared to that of the base fluid:

➕ **Maxwell model :**

The effective thermal conductivity of the nanofluid is approximated by the Maxwell auto-coherent approximation model. For the two-component entity of the spherical particle suspension .The model of Maxwell (1873) is given by the following formula:

$$\lambda_{eff} = \frac{\lambda_p + 2\lambda_{bf} + 2\varphi(\lambda_p - \lambda_{bf})}{\lambda_p + 2\lambda_{bf} - \varphi(\lambda_p - \lambda_{bf})} \lambda_{bf} \qquad \text{(I.7)}$$

Where λ_p the thermal conductivity of the particles is, λ_{eff} is the effective thermal conductivity of Nano fluid, λ_{bf} is the base fluid thermal conductivity, and φ is the volume fraction of the suspended particles[6].

The Hamilton-Crosser model and the Yu-Choi model, which consider the spherical form of nanoparticles:

🔸 Hamilton & Crosser Model (1962):

The Hamilton and Crosser model was established to resolve the Maxwell model limit. Since the latter only applies to spherical particles. The apparent thermal conductivity of the medium is given by the following expression:

$$\lambda_{eff} = \frac{\lambda_p + (n-1)\lambda_{bf} - (n-1)(\lambda_{bf} - \lambda_p)\varphi}{\lambda_p + (n-1)\lambda_{bf} + \varphi(\lambda_{bf} - \lambda_p)} \lambda_{bf} \qquad \textbf{(I.8)}$$

Or (n) is an empirical form factor given by$= \frac{3}{\Psi}$.

n=3 for spherical particles and n-6 for cylindrical particles.

For (Ψ=1) (spherical particles) the Hamilton and Crosser model is identical to the Maxwell model.

🔸 Yu and Choi Model:

Another expression for calculating thermal conductivity was introduced by Yu and Choi (2003) .They proposed to model Nanofluids as a basic liquid and solid particles separated by a nanometric layer, this layer acts

$$\frac{\lambda_{eff}}{\lambda_{bf}} = \frac{\lambda_p + 2\lambda_{bf} - 2(1+\beta)^3(\lambda_{bf} - \lambda_p)\varphi}{\lambda_p + 2\lambda_{bf} + 2(1+\beta)^3(\lambda_{bf} - \lambda_p)\varphi} \qquad \textbf{(I.9)}$$

β: Ratio of the thickness of the nanometer layer to the particle radius.

I.4.6 Viscosity

Viscosity is an important factor for thermal applications involving fluids. In addition, heat transfer by convection is influenced by viscosity. As a result, viscosity requires the same attention as thermal conductivity because of its very significant impact on heat transfer. The viscosity of nanofluids increases mainly by increasing the concentration of nanoparticles and decreases by raising the temperature. Several viscometers with various functional bases have been employed to measure the viscosity of nanofluids, such as the capillary tube viscometer, Vibro viscometer, rotational rheometer, drop/fall ball, piston viscometer, and cup viscometer. Among others, the rotary rheometer, piston rheometer, and capillary tube viscometer are the most commonly used devices for viscosity measurements of nanofluids. Moghaddam et al. prepared graphene and glycerol-based nanofluids and performed experimental measurements of the rheological properties of the nanofluids. These results indicate that the viscosity of graphene-glycerol nanofluids is dependent on mass fraction and temperature. The viscosity improves with increasing mass fraction and decreases with increasing temperature. In this investigation, the 401.49% increase in viscosity of glycerol was obtained by loading 2% of graphene Nano sheets at a shear rate of 6.32 s−1 and 20 °C. Einstein studied the dynamic viscosity of a Nanofluid for a mixture consisting of dilute suspensions of fine, spherical particles.

The expression that characterizes this model is the following [6]:

$$\mu_{nf} = \mu_{bf}(1 + 2.5\varphi)$$ **(I.10)**

With μ_{nf} and μ_{f} are respectively the dynamic viscosities of the Nanofluid, the base fluid and φ the volume fraction of the nanoparticles.

✦ Brinkman model :

Later, brinkman (1952) presented a viscosity correlation that extended Einstein's equation to suspensions with moderate particle volume fraction, typically less than 4%

$$\mu_{nf} = \frac{\mu_{bf}}{(1-\varphi)^{2.5}}$$ **(I.11)**

▪ Batchelor model :

The effect of Brownian motion on the effective viscosity in a suspension of rigid spherical particles was studied by Batchelor (1977) for isotropic structure of suspension, the effective viscosity was given by:

$$\mu_{eff} = (1 + 2.5\varphi + 6.2\varphi^2)\mu_{bf} \tag{I.12}$$

I.5 Heat transfer applications:

- **Industrial Cooling Applications**: **Routbort et al. [9]** started a project in 2008 that employed nanofluids for industrial cooling that could result in great energy savings and resulting emissions reductions. For U.S. industry, the replacement of cooling and heating water with nanofluids has the potential to conserve 1 trillion Btu of energy. For the U.S. electric power industry, using nanofluids in closed loop cooling cycles could save about 10–30 trillion Btu per year (equivalent to the annual energy consumption of about 50,000–150,000 households). The associated emissions reductions would be approximately 5.6 million metric tons of carbon dioxide; 8,600 metric tons of nitrogen oxides; and 21,000 metric tons of sulfur dioxide.

- For Michelin North America tire plants, the productivity of numerous industrial processes is constrained by the lack of facility to cool the rubber efficiently as it is being processed. This requires the use of over 2 million gallons of heat transfer fluids for Michelin's North American plants. It is Michelin's goal in this project to obtain a 10% productivity increase in its rubber processing plants if suitable water-based nanofluids can be developed and commercially produced in a cost-effective manner.

- **Han et al**. **[10]** have used phase change materials as nanoparticles in nanofluids to simultaneously enhance the effective thermal conductivity and specific heat of the fluids. As an example, a suspension of indium nanoparticles (melting temperature, 157◦C) in polyalphaolefin has been synthesized using a one-step, nano emulsification method. The fluid's thermophysical properties, that is, thermal conductivity, viscosity, and specific heat, and their temperature dependence were measured experimentally. The observed melting-freezing phase transition of the indium nanoparticles significantly augmented the fluid's effective specific heat. This work is one of the few to address thermal diffusivity; similar studies allow industrial cooling applications to continue without thorough understanding of all the heat transfer mechanisms in nanofluids.

I.6 Uses of nanofluid

Nano fluids can be used to improve heat transfer and energy efficiency across multiple thermal systems. Here are a few examples of applications:

- **Cooling thermal systems**:

The mixture of ethylene glycol and water, are used as coolant in the engines of vehicles, and the addition of nanoparticles in these liquids improves the cooling rate. This point is studied by several groups of researchers; Tzeng and Col have dispersed AL203 and CuO nanoparticles in engine cooling oil[11].

- **Cooling of electronic systems:**

In integrated circuits, nano-fluids have been considered as cooling fluids, for which several studies have been for this purpose several studies have been carried out. Tsai et al used a water-based nanofluid to cool a central processing unit in a computer[11].

- **Cooling of military systems:**

Examples of military applications include cooling of power electronics and directed energy weapons. These involve very high heat fluxes (q>500 to 1000 W/cm2) where nano-fluids have been shown to be effective in cooling these systems, and also other military systems including military vehicles, submarines and high power laser diodes[11].

- **Cooling of space systems:**

For applications in space. You et al and Vassallo et al have performed studies to show that the presence of studies to show that the presence of nanoparticles in the cooling fluid in general electronics plays a very important role in space applications where the power density is very power density is very high.

- **Cooling of nuclear systems:**

The Massachusetts Institute of Technology has set aside an interdisciplinary center solely for new nanotechnology (nano-fluid) in the nuclear power industry. Currently, they are evaluating the potential impact of nano-fluid use on the safety economic performance of nuclear systems.
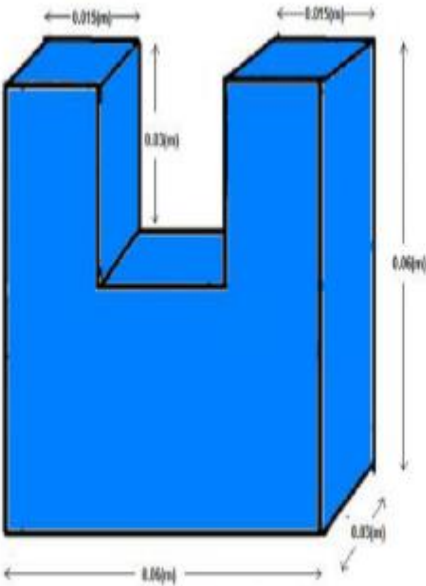
- **Biomedicine:**

Nano-fluids and nanoparticles have many applications in biomedicine. For example, to avoid some side effects of traditional cancer treatment methods, iron-based nanoparticles have been used as drug carriers. Also for safer surgery by producing effective cooling around the surgical area, Jordan et al. surgical area, Jordan et al.

I.7 Example applications of nanofluids

In this is an example about nanofluid application:

Table (I.6): An example of applications of nanofluid in heat transfer.

Author	Année	Parameter	Method
Soufi El Habib. [8]	**2013**	φ=0.01-0.15 Ra=103-106	Volumes Finis
Configuration		**Observation**	

<table>
<tr>
<td>

Schéma 1 : la cavité en forme U.

</td>
<td>

The use of nanofluids to increase heat transfer in natural convection is considered as a novel technique that can meet the demands of the industry in an efficient manner. The results obtained from the numerical study of the effects of variation of the volume fraction and the Rayleigh number on the performance of heat transfer of a nanofluid (Al2O3-water).

-Increased nanofluid density fraction and Rayleigh number can improve the performance of convective heat transfer in a given geometric cavity.

The nanofluid is a favorable fluid for cooling systems by supplying the other fluid (the base fluids).

</td>
</tr>
</table>

I.8 how can a nanofluid improve heat transfer?

To improve performance, the thickness of the boundary layer must be reduced as much as possible and prevented from growing as much as possible. and prevent it from developing as it pleases. To do this, we increase the speed of the fluid (narrow passages, water jets...) or by placing small obstacles (peaks, roughness...) to increase the mixing at the level of the wall in particular. All this to counteract it as much as possible and push the cold fluid as close as possible to the hot wall to increase the exchange the exchange decrease of the thickness of the thermal boundary layer. Thanks to its higher thermal conductivity, a nanofluid directly improves the transit of thermal energy through the viscous sublayer. The suspension of nanoparticles can significantly modify the rheological behavior of the liquid by adopting a particular structural arrangement in the boundary layer. Depending on their nature and shape, one can observe a rheofluid can be observed a rheofluidizing behavior (decrease of viscosity when the shear rate increases) which tends to reduce the apparent viscosity near the wall (lubricating effect).

This reduction in viscosity induces a decrease in the thickness of the dynamic boundary layer and therefore thermal by implication. The result is once again a direct increase of the exchange coefficient at the wall [12].

I.9 The advantages and disadvantages of Nano fluid

I.9.1 The advantages of Nano fluid

- The advantage of using Nano-fluids as heat transfer fluids strongly depends on a trade-off between increased thermal conductivity (determining in the intensification of convective heat transfer) and increased viscosity (determining the undesirable increase in pumping power). Future research should therefore be directed towards the selection of materials, shape and size of nanoparticles that would increase the thermal conductivity of the mixture with a moderate increase in viscosity.

- A large heat transfer surface between particles and fluids.

- Reduced clogging particles compared to conventional sludge, thus favoring system miniaturization.

- Adjustable properties, including thermal conductivity and wettability of the surface, by varying concentrations of [articulates according to different applications[13].

I.9.2 the disadvantages of Nano fluid

- Lack of agreement on the results obtained by different researchers.
- Lack of theoretical understanding of the mechanisms responsible for changes in properties
- Poor characterization of suspensions.
- Stability of nanoparticles dispersion.
- Increased pressure drop and pumping power.
- Higher viscosity, specific heat Low.
- The high cost of nano-fluids.
- Difficulties in the production process[13].

I.10 Conclusion

It is important to note that preparation of nanofluids is an important step in experiments on nanofluids. Having successfully engineering the nanofluids, the estimation of thermo physical properties of nanofluids captures the attention. Great quanta of attempts have been made to exactly predict them but large amount of variations were found. Research works on convective heat transfer using nanofluids is found to increase exponentially in the last decade. Almost all the works showed that the inclusion of nanoparticles into the base fluids has produced a considerable augmentation of the heat transfer coefficient that clearly increases with an increase of the particle concentration. It was reported by many of the researchers that the increase in the effective thermal conductivity and huge chaotic movement of nanoparticles with increasing particle concentration is mainly responsible for heat transfer enhancement. However, there exists aplenty of controversy and inconsistency among the reported results. The outcome of all heat transfer works using nanofluids showed that our current understanding on nanofluids is still quite limited. There are a number of challenges facing the nanofluids community ranging from formulation, practical application to mechanism understanding. Engineering suitable nanofluids with controlled particle size and morphology for heat transfer applications is still a big challenge. Besides thermal conductivity effect, future research should consider other properties, especially viscosity and wettability, and examine systematically their influence on flow and heat transfer. An in-depth understanding of the interactions between particles, stabilizers, the suspending liquid and the heating surface will be important for applications.

CHAPTER II

GEOMETRY AND MATHEMATIC MODELING

II.1 Introduction:

The study of a physical phenomenon calls for the elaboration of laws in the form of mathematical equations coupling of the various variables implicated in the evolution of the phenomenon [1]. Generally speaking, these equations are: the continuity equation that reflects the principle of mass preservation, Navier-Stokes equations which reflect the principle of momentum conservation, and the energy equation which represents the principle of energy conservation. The description of a given problem also requires the definition of a certain number of boundary conditions.

II.2 The geometry of the studied problem:

II.2.1The description of the problem:

The plot of the model under consideration is shown in the Figure (II-1) with coordinates system. A two-dimensional inclined square cavity containing a Nano-fluid. The left and the right walls are kept respectively at hot and cold temperature (T_h, T_c). The upper and lower horizontals walls are insulated. It is assumed that nanoparticles and the base fluid are in thermal equilibrium and there is no slippage between them. The thermo-physical properties of the Nano-fluid are considered constant with the exception of the density which varies according to the Boussinesq approximation.
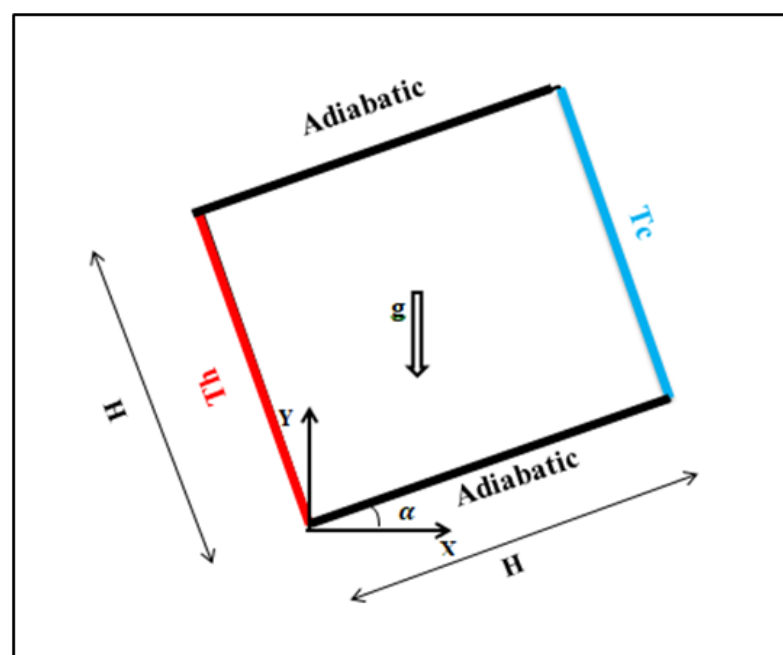
Figure (II.1): Geometry of the studied model.

II.3 Simplifying hypothesis:

The resolution of governing equations requires a number of simplifying hypotheses, admittedly:

- Newtonian and incompressible fluid.

- Two-dimensional flow in Cartesian coordinates ($\frac{\partial}{\partial z} = 0$).

- Laminar and permanent flow rate ($\frac{\partial}{\partial t} = 0$).

- Absence of mass source and chemical reaction.

- Heat transfer by radiation is negligible.

- The energy induced by the viscous forces is negligible($\emptyset = 0$).

II.4 Mathematical formulation of the problem:

The mathematical formulation for convective phenomena depends on equations that link the various parameters, namely: velocity, pressure and temperature. These equations are obtained in special cases from the following general equations (continuity, momentum, and energy equations):

II.4.1 Continuity equation:

The continuity equation is simply a mathematical expression of the principle of conservation of mass. For a control volume that has a single inlet and a single outlet, the principle of conservation of mass states that, for steady-state flow, the mass flow rate into the volume must equal the mass flow rate out. The continuity equation for this situation is expressed by:

$$\frac{\partial \rho}{\partial t} + \text{div}(\rho \vec{V}) = 0 \qquad \text{(II.1)}$$

$$\vec{V} = u\vec{\imath} + v\vec{\jmath} + w\vec{k}$$

For an incompressible $div\vec{V} = 0$

II.4.2 The momentum conservation equation:

The second law of dynamics indicates that the rate of variation in quantity of movement contained in the control volume is equal to the sum of all external forces applied to it. It is written in the following form:

$$\rho \frac{d\vec{V}}{dt} = -\frac{dP}{dX} + \rho\vec{g} + \mu \, \Delta\vec{V} \tag{II.2}$$

Where: $\vec{g}$ is the gravity, P is the pressure and $\mu\Delta\vec{V}$ is the viscosity forces (stresses).

II.4.3 Energy conservation equation:

The energy conservation equation is obtained from the first principle of thermodynamics and it can be written as:

$$\rho Cp \frac{dT}{dt} = div\left(\lambda \overrightarrow{grad}T\right) + T\beta \frac{dp}{dt} + q + \phi \tag{II.3}$$

q: is the internal source (chemical reaction, etc.)

ϕ: is the dissipation function grouping all terms containing viscosityμ.

➢ For the incompressible fluid, it is written in the following form:

$$\rho C_P \left(\frac{dT}{dt} + u\,\frac{\partial T}{\partial x} + v\,\frac{\partial T}{\partial y} + w\,\frac{\partial T}{\partial z}\right) = \lambda \left(\frac{d^2T}{dx^2} + \frac{d^2T}{dy^2} + \frac{d^2T}{dx^2}\right) + \phi \tag{II.4}$$

II.5 Problem formulation:

II.5.1 Dimensional problem formulation:

In the two-dimensional laminar steady state, the equations of continuity, momentum and energy for convection fluid flow and heat transfer are written as follows:

$$\frac{\partial U}{\partial X} + \frac{\partial V}{\partial Y} = 0 \tag{II.5}$$

$$\rho_{nf} \left[u\frac{\partial u}{\partial x} + v\frac{\partial u}{\partial y}\right] = -\frac{\partial P}{\partial x} + \mu_{nf}\left(\frac{\partial^2 u}{\partial x^2} + \frac{\partial^2 u}{\partial y^2}\right) - \rho g_x \tag{II.6}$$

$$\rho_{nf} \left[u\frac{\partial v}{\partial x} + v\frac{\partial v}{\partial y}\right] = -\frac{\partial P}{\partial y} + \mu_{nf}\left(\frac{\partial^2 v}{\partial x^2} + \frac{\partial^2 v}{\partial y^2}\right) - \rho g_y \tag{II.7}$$

$$(\rho C_P)_{nf} \left[u\frac{\partial T}{\partial x} + v\frac{\partial T}{\partial y}\right] = \lambda_{nf}\left(\frac{\partial^2 T}{\partial x^2} + \frac{\partial^2 T}{\partial y^2}\right) \tag{II.8}$$

I.5.2 Boussinesq approximation:

The Boussinesq approximation is an approximation used in fluid mechanics that assumes that the fluid density is constant except for thermal expansion. Thus, centrifugal and gravitational forces can be estimated using a constant value for density, rather than calculating it precisely using the equation of state.

The Boussinesq approximation can be applied in the above equations by replacing ρ with a constant ρ_0 in all terms, except for terms involving thermal expansion, where the coefficient of thermal expansion β is used to estimate the change in density due to changes in temperature.

$$\rho = \rho_0[1 - \beta(T - T_0)] \tag{II.9}$$

With:

T_0: The reference temperature.

ρ_0 **:** The density of the fluid in T_0.

β**:** The thermal volume expansion coefficient of the fluid given by :

$$\beta = -\frac{1}{\rho}\left(\frac{\partial P}{\partial T}\right)_P \tag{II.10}$$

I.5.3 Simplified equations:

➢ **Continuity equation:**

$$\frac{\partial u}{\partial x} + \frac{\partial v}{\partial y} = 0 \tag{II.11}$$

➢ **The momentum conservation equation:**

- **On (ox):**

$$u\frac{\partial u}{\partial x} + v\frac{\partial u}{\partial y} = -\frac{1}{\rho_{nf}}\frac{\partial P}{\partial x} + \vartheta_{nf}\left(\frac{\partial^2 u}{\partial x^2} + \frac{\partial^2 u}{\partial y^2}\right) + g\beta_{nf}(T - T_0)\sin\alpha \tag{II.12}$$

- **On (oy):**

$$u\frac{\partial v}{\partial x} + v\frac{\partial v}{\partial y} = -\frac{1}{\rho_{nf}}\frac{\partial P}{\partial y} + \vartheta_{nf}\left(\frac{\partial^2 v}{\partial x^2} + \frac{\partial^2 v}{\partial y^2}\right) + g\beta_{nf}(T - T_0)\cos\alpha \tag{II.13}$$

> ➤ **Energy conservation equation:**

$$u\frac{\partial T}{\partial x} + v\frac{\partial T}{\partial y} = \alpha_{nf}\left(\frac{\partial^2 T}{\partial x^2} + \frac{\partial^2 T}{\partial y^2}\right)$$

(II.14)

I.5.4 Boundary conditions:

$$\begin{cases} x = 0 : u = v = 0 , \quad T = T_h \\ x = H : u = v = 0 , \quad T = T_c \end{cases} \begin{cases} y = 0 : u = v = 0 , \quad \dfrac{\partial T}{\partial y} = 0 \\ y = H : u = v = 0 , \quad \dfrac{\partial T}{\partial y} = 0 \end{cases}$$

II.6 Dimension-less problem formulation:

We apply the same simplification hypotheses as the previous state. Experimental studies of the flows are often carried out on models and the results are shown in dimensions without form, thus allowing measures to be staggered towards the real conditions of the flows. The same approach can also be undertaken in digital studies. The governing equations can be transformed into the dimensionless form by using appropriate normalization [1].

Using the following dimension-less parameters, the override warning can be converted to a dimension-less shape:

$$X = \frac{x}{H} \;;\; Y = \frac{y}{H} \;;\; U = \frac{uH}{\alpha_f} \;;\; V = \frac{vH}{\alpha_f} \;;\; P = \frac{pH^2}{\rho_{nf}\alpha_f^2} \;;\; \theta = \frac{T - T_c}{T_h - T_c}$$

$$x = XH \;,\; y = YH \;,\; u = \frac{U\,\alpha_f}{H} \;,\; v = \frac{V\,\alpha_f}{H} \;,\; p = \frac{H^2}{\rho_{nf}\alpha_f^2} \;,\; T = \theta(T_h - T_c) + T_c$$

> ➤ **Continuity equation:**

$$\frac{\partial U}{\partial X} + \frac{\partial V}{\partial Y} = 0$$

(II.15)

> ➤ **Momentum equation:**

On x:

$$\frac{\partial U}{\partial t} + U\frac{\partial U}{\partial X} + V\frac{\partial U}{\partial Y} = -\frac{\partial P}{\partial X} + \frac{\mu_{nf}}{\rho_{nf}\alpha_f}\left[\frac{\partial^2 U}{\partial X^2} + \frac{\partial^2 U}{\partial Y^2}\right] + \frac{(\rho\beta)_{nf}}{\rho_{nf}\beta_f}\,\mathrm{Ra.\,Pr.\,\theta.\sin(\alpha)}$$

(II.16)

On y:

$$\frac{\partial V}{\partial t} + U\frac{\partial V}{\partial X} + V\frac{\partial V}{\partial Y} = -\frac{\partial P}{\partial Y} + \frac{\mu_{nf}}{\rho_{nf}\alpha_f}\left[\frac{\partial^2 V}{\partial X^2} + \frac{\partial^2 V}{\partial Y^2}\right] + \frac{(\rho\beta)_{nf}}{\rho_{nf}\beta_f}\text{Ra}.\,\text{Pr}.\,\theta.\cos(\alpha) \qquad \textbf{(II.17)}$$

➢ **Energy equation:**

$$\frac{\partial\theta}{\partial t} + U\frac{\partial\theta}{\partial X} + V\frac{\partial\theta}{\partial Y} = \frac{\alpha_{nf}}{\alpha_f}\left[\frac{\partial^2\theta}{\partial X^2} + \frac{\partial^2\theta}{\partial Y^2}\right] \qquad \textbf{(II.18)}$$

Where the density, coefficient of thermal expansion, calorific power and thermal diffusivity of the nano-fluid are respectively:

$$\rho_{nf} = (1-\varphi)\rho_f + \varphi\rho_p \qquad \textbf{(II.19)}$$

$$(\rho C_P)_{nf} = (1-\varphi)(\rho C_P)_f + \varphi(\rho C_P)_p \qquad \textbf{(II.20)}$$

$$(\rho\beta)_{nf} = (1-\varphi)(\rho\beta)_f + \varphi(\rho\beta)_p \qquad \textbf{(II.21)}$$

$$\alpha_{nf} = \frac{\lambda_{nf}}{(\rho C_P)_{nf}} \qquad \textbf{(II.22)}$$

To estimate the dynamic viscosity of the nano-fluid, the Brinkman model is used:

$$\mu_{eff} = \frac{\mu_{nf}}{(1-\varphi)^{2.5}} \qquad \textbf{(II.23)}$$

The effective thermal conductivity of the nano-fluid is determined according to Maxwell:

$$\lambda_{eff} = \frac{\lambda_p + 2\lambda_{bf} - 2\varphi(\lambda_p - \lambda_{bf})}{\lambda_p + 2\lambda_{bf} + \varphi(\lambda_p - \lambda_{bf})} \qquad \textbf{(II.24)}$$

With:

➢ Rayleigh number : $Ra = \frac{g\beta_f\Delta T H^3}{\upsilon_f\alpha_f}$

➢ $\Delta T = T_h - T_c$

➢ Prandtl number : $Pr = \frac{\vartheta_{nf}}{\alpha_{nf}}$

➢ Cinematic viscosity : $\vartheta_{nf} = \frac{\mu_{nf}}{\rho_{nf}}$

II.6.1 Dimensionless Boundary conditions

➢ $\begin{cases} X = 0 : U = V = 0,\ \theta = 1 \\ X = 1 : U = V = 0,\ \theta = 0 \end{cases} \begin{cases} Y = 0 : U = V = 0,\ \frac{\partial\theta}{\partial y} = 0 \\ Y = 1 : U = V = 0,\ \frac{\partial\theta}{\partial y} = 0 \end{cases}$

II.7 Dimensionless numbers

II.7.1 Prandtl number:

Which is the ratio of kinematic viscosity ϑ_{nf} and thermal diffusivity α_{nf}, it characterizes the relative importance of thermal and viscous effects, this number is named after Ludwig Prandtl, German physicist, Prandtl number is therefore the ratio of two magnitudes with the same dimensions, that is (m^2/s)

The Prandtl number compares the speed of thermal and hydrodynamic phenomena in a fluid. A high Prandtl number indicates that the temperature profile in the fluid will be strongly influenced by the velocity profile. A low Prandtl number indicates that the heat conduction is so fast that the velocity profile has little effect on the temperature profile. Is given by the expression:

$$Pr = \frac{\vartheta_{nf}}{\alpha_{nf}}$$
(II.25)

II.7.2 Rayleigh number

$$Ra = \frac{g\beta_f \Delta T H^3}{\upsilon_f \alpha_f} = G_r . P_r$$
(II.26)

The Rayleigh number is directly related to convection. Convection occurs when buoyancy (due to the increase in temperature) creates the motion of the fluid. However, this buoyancy must be large enough to counteract the viscous forces that oppose the motion of the particle. Moreover, if thermal equilibrium is reached, there is no longer any Archimedean force. The ability of a particle to come into equilibrium with its environment more or less quickly depends on its thermal diffusivity (α) Ra gives us the ratio of the time for the heat to diffuse to the time for the particle to come into motion.

II.7.3 Nusselt number

It is the ratio of the temperature gradient in the fluid in immediate contact with the surface to the reference temperature gradient. It characterizes the intensity of heat exchange on the fluid-surface boundary.

$$Nu = \frac{h.H}{\lambda_f}$$
(II.27)

Local Nusselt number :

- **The left wall:**

$$\emptyset_{cond} = \emptyset_{conv}$$

$$-\lambda_{nf} \frac{\partial T}{\partial X})_{x=0} = h\, \Delta T$$

$$h = \frac{-\lambda_{nf}}{\Delta T} \frac{\partial T}{\partial X}$$

$$Nu = \frac{-\lambda_{nf}}{\lambda_f \Delta T} \frac{\partial T}{\partial X}\, H$$

$$Nu_{nf} = \frac{\lambda_{nf}}{\lambda_f} \frac{\partial \theta}{\partial X}$$

- **The right wall:**

$$-\lambda_{nf} \frac{\partial T}{\partial X})_{x=H} = h\, \Delta T$$

$$Nu_{nf} = \frac{-\lambda_{nf}}{\lambda_f} \frac{\partial \theta}{\partial X}$$

Average Nusselt number :

$$\overline{Nu} = \frac{1}{H}\int_{0}^{1} Nu\, \partial y$$

$$\overline{Nu} = \frac{1}{H}\int_{0}^{1} \frac{-\lambda_{nf}}{\lambda_f} \frac{\partial \theta}{\partial X}\, \partial y$$

II.8 Conclusion

In this chapter, we have presented the physical model in question as well as the equations that govern the studied phenomenon with its boundary conditions.

CHAPTER III

NUMERICAL AND MATHEMATIC FORMULATION MODELING

III.1   Introduction

Solving the equations of a physical phenomenon of natural thermal convection is done by using a numerical method. The latter consists in developing the means of solving these equations. At this stage, the concept of discretization comes into play. The result of the discretization of differential transport equations is a system of nonlinear algebraic equations; these equations describe the discrete properties of fluid to nodes in the solution domain.

There are several numerical methods for discretizing differential partial differential equations, namely:

* The finite element method.

* The finite differences method.

* The finished volume method.

In this study, the finite volume method with quadrilateral control volumes will be used.

The discretization scheme used is polynomial and the speed-pressure coupling is calculated according to the SIMPLE algorithm developed by Spalding and Patankar [15].

III.2   Reminders on the finite volume method

Using this method, the computation domain is divided into a finite number of elementary subdomains called control volumes. The finite volume method consists of integrating equations with partial derivatives on each control volume. Each of these includes a node known as the main node, as shown in Figure (III.2).

The finite volume method essentially consists of:

• The discretization of the domain considered in control volumes.

 • The integral formulation of partial differential equations.

• The model must be stable and convergent.

A discretization technique converts conservation equations to partial derivatives into algebraic equations that can be solved numerically. The computation domain is divided into a finite number of elementary subdomains, called control volume, each of which includes a node called the main node. The control volume technique consists in the integration of partial differential equations on

each control volume to obtain discretized equations that retain all physical quantities on a control volume.

This method will be applied on the transport equation, which can be written in the following general form:

$$\frac{\partial}{\partial t}(\rho\varphi) + div\big(\Gamma grad(\varphi)\big) + S\varphi \qquad \textbf{(III.1)}$$
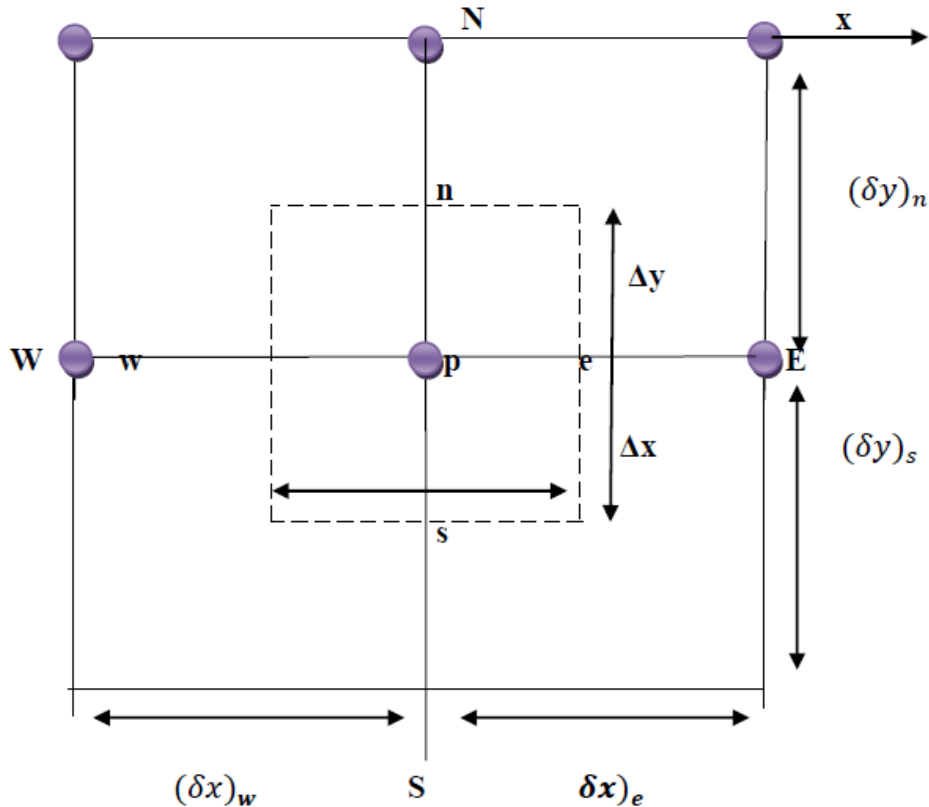
Figure (III.1): two-dimensional Control Volume.

III.2.1 Mesh

The point differential equations that govern our phenomenon are written in every point of the physical domain. To project them on this domain we build a grid divided into a certain number of finite volumes, and in each volume, we consider points in the middle. The faces of a typical control volume are located at the point e, w, n, s (**Figure III.2).** Note P the center of the control volume considered and E, W, N, S are the centers of the adjacent control volumes located respectively to the east, west, north and south of that containing P. Scalar quantities (pressure and temperature) are stored at the centers of the finished volumes (**Figure III.2).** On the other hand, vector quantities (components u and v) are stored on the east and north faces respectively **(a), (b)**

and (**c**). To avoid some numerical problems, motion quantity equations are solved in right-shifted finite volumes for the next X pulse and up for the next Y pulse **[16].**

(a)   (b)

(c)
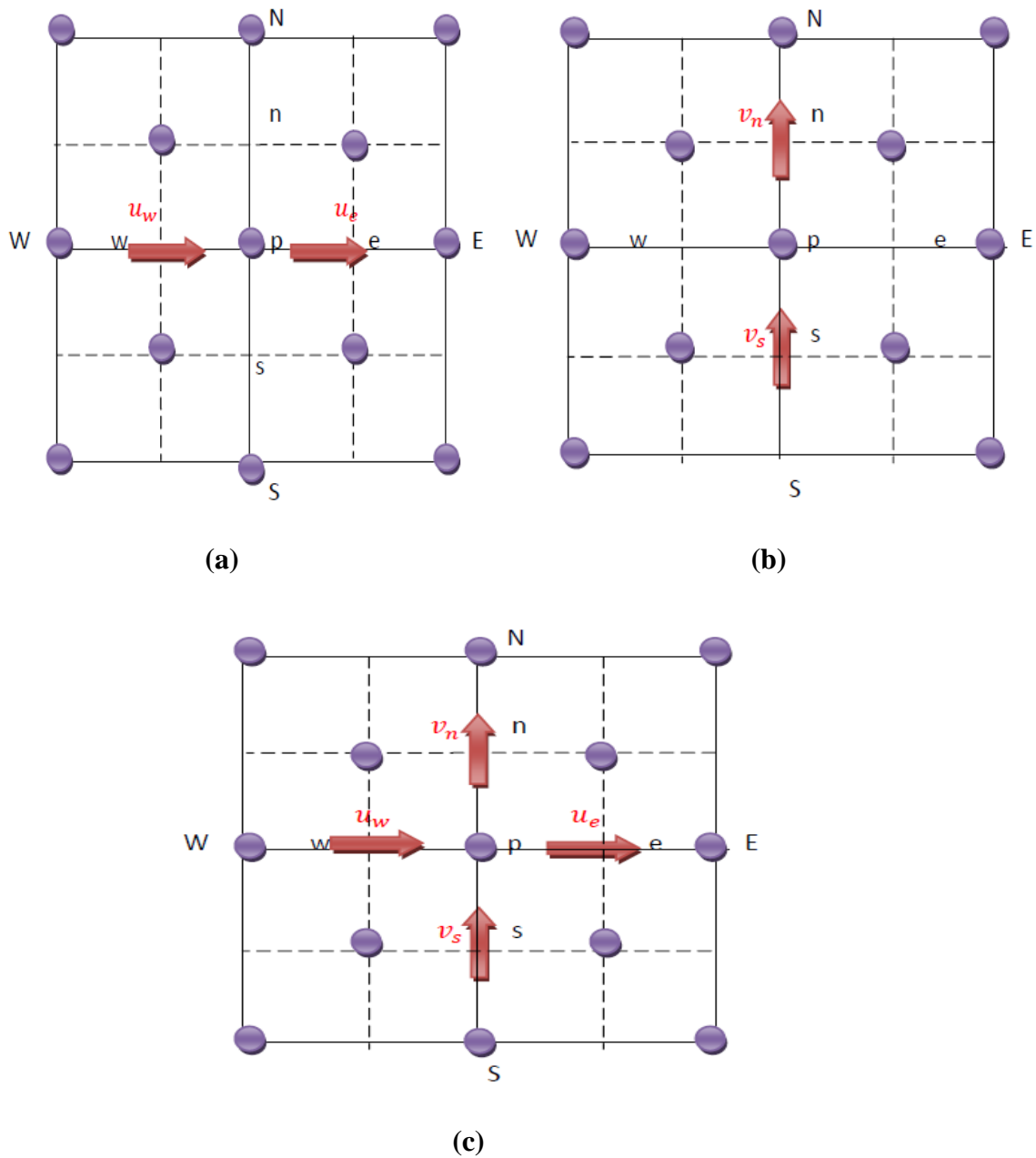
Figure (III.4): Control volume diagram (c), offset mesh for u_e (a), offset mesh for v_e (b)

III.3 General Transport equation

With:

$$\frac{\partial \varphi}{\partial t} + div(\vec{V}\emptyset) = \Gamma(\nabla^2\emptyset) + S_\varphi \tag{III.2}$$

[1]   [2]   [3]   [4]

33

[1]: Transitional term;

[2]: Term of convection;

[3]: Term of dissemination;

[4]: Source term;

　　　We have just seen that for each variable ϕ, the transport equation is written in the stationary, two-dimensional case as follows:

Table (III.I): variables and coefficients of dimensionless transport equations.

equation	$\emptyset$	Γ	$S_\emptyset$
continuity	1	0	0
Motion in the direction (ox)	U	$\dfrac{\mu_{nf}}{\rho_{nf}\alpha_f}$	$-\dfrac{\partial P}{\partial X} + \dfrac{(\rho\beta)_{nf}}{\rho_{nf}\beta_f} R_a P_r \theta \sin\alpha$
Motion in the direction (oy)	V	$\dfrac{\mu_{nf}}{\rho_{nf}\alpha_f}$	$-\dfrac{\partial P}{\partial Y} + \dfrac{(\rho\beta)_{nf}}{\rho_{nf}\beta_f} R_a P_r \theta \cos\alpha$
Energy	θ	$\dfrac{\alpha_{nf}}{\alpha_f}$	**0**

III.3.1 Discritization of the general transport equations

By integrating the general transport equation on a typical control volume (Figure III.1) $\Delta V = \Delta X . \Delta Y . 1$ and in the time interval t and (t+Δt) in a two-dimensional Cartesian domain.

$$\oint \left[\frac{\partial \emptyset}{\partial x} + div(\vec{V} \emptyset) \right] dXdYdT = \oint (\Gamma (\nabla^2 \emptyset) + S_\emptyset) dXdYdT \qquad \textbf{(III.3)}$$

$$\int_t^{t+\Delta t} \int_s^n \int_w^e \frac{\partial \emptyset}{\partial T} dXdYdT + \int_t^{t+\Delta t} \int_s^n \int_w^e \frac{\partial J_x}{\partial T} dXdYdT + \int_t^{t+\Delta t} \int_s^n \int_w^e \frac{\partial J_y}{\partial T} dXdYdT = \int_t^{t+\Delta t} \int_s^n \int_w^e S_\emptyset \, dXdYdT$$

By posing:

$$J_x = U\emptyset - \Gamma \frac{\partial \emptyset}{\partial X} \qquad \text{And} \qquad J_y = V\emptyset - \Gamma \frac{\partial \emptyset}{\partial Y}$$

J_x J_y : The differences between the convective and diffusive flows respectively in the direction equation (III.1) is written as follows:

$$\frac{\partial \emptyset}{\partial T} + \frac{\partial J_x}{\partial X} + \frac{\partial J_y}{\partial Y} = S \qquad \textbf{(III.4)}$$

To be able to approximate the equation in algebraic form, we consider the hypotheses following:

- The generalized variable. Varies linearly the main nodes in both directions
- The convective and diffusive terms are uniform across the corresponding faces.
- The source term is uniform on the control volume

The transitional term:

$$\int_t^{t+\Delta t} \int_s^n \int_w^e \frac{\partial \emptyset}{\partial T} dXdYdT = \left[\emptyset_p^{t+\Delta t} - \emptyset_p^t \right] \Delta X \Delta Y = \emptyset_p^{t+\Delta t} \Delta X \Delta Y - \emptyset_p^t \Delta X \Delta Y$$

(III.5)

The total flow term:

$$\int_t^{t+\Delta t} \int_s^n \int_w^e \frac{\partial J_x}{\partial T} dXdYdT = [J_e - J_w] \Delta Y \Delta T = J_e \Delta Y \Delta T - J_w \Delta Y \Delta T$$

(III.6)

$$\int_t^{t+\Delta t} \int_s^n \int_w^e \frac{\partial J_x}{\partial T} dXdYdT = [J_n - J_s] \Delta X \Delta T = J_n \Delta X \Delta T - J_s \Delta X \Delta T$$

(III.7)

If we assume:

$$j_e = J_e \Delta Y \qquad j_w = J_w \Delta Y$$

$$j_n = J_n \Delta X \qquad j_s = J_s \Delta X$$

The quantities $\boldsymbol{j_e}, \boldsymbol{j_w}, \boldsymbol{j_n}$ and $\boldsymbol{j_s}$ are the flows at the interfaces *(e, w, n,* and *s)*.

The source term:

$$\int_t^{t+\Delta t} \int_s^n \int_w^e S_\emptyset \, dX dY dT = \overline{S_\emptyset} \Delta X \Delta Y \Delta T$$

(III.8)

The source term $\overline{S_\emptyset}$ in each conservation equation must be linearized so that the whole system of equations take the linear form and the resolution becomes simplified. So the term $\overline{S_\emptyset}$ can be put in the following form: $\overline{S_\emptyset} = S_c + S_p \emptyset_p$

S_p Must be negative in order to meet the rules of the finite volume method (Patankar 1980), and thus facilitate the convergence of the system (the diagonal of the matrix of the system to be solved becomes dominant).

It is necessary that the coefficient S_p is less than zero for the solution to be numerically stable and convergence to be faster

S_p: is the coefficient of $\emptyset_p$

S_c:is the constant part that does not depend on $\emptyset_p$

So:

$$\frac{\emptyset_p^{t+\Delta t} - \emptyset_p^t}{\Delta T} \Delta X \Delta Y + (j_e - j_w) + (j_n - j_s) = \overline{S_\emptyset} \Delta X \Delta Y \qquad \textbf{(III.9)}$$

All flows are evaluated at time $(T + \Delta T)$

In order to completely establish the discretize form of the general transport equation, integrating the continuity equation:

$$\int_s^n \int_w^e \frac{\partial U}{\partial X} dX dY + \int_s^n \int_w^e \frac{\partial V}{\partial Y} dX dY = 0$$

(III.10)

We obtain:

$$(U_e - U_w)\Delta Y + (U_n - U_s)\Delta X = 0$$
(III.11)

The convective flow is defined through the faces of the control volume by:

$$F_e = U_e \Delta Y \qquad F_w = U_w \Delta Y$$

(III.12)

$$F_n = U_n \Delta X \qquad F_s = U_s \Delta X$$

By replacing these flows with their expressions in equation (III.11) we obtain:

$$(F_e - F_w) + (F_n - F_s) = 0$$

(III.13)

We add the equation (III.9) to the product of equation (III.13) by $\emptyset_p$ we will have :

$$\frac{\emptyset_p^{t+\Delta t} - \emptyset_p^t}{\Delta T} \Delta X \Delta Y + (j_e - F_e \emptyset_P) - (j_w - F_w \emptyset_P) + (j_n - F_n \emptyset_P) - (j_s - F_s \emptyset_P) = \overline{S_\emptyset} \Delta X \Delta Y$$

(III.14)

Expressions in parenthesis can be put in the common form, presented by Patankar.

As substituting these expressions in equation (III.14), the general equation discretize in time, makes it possible to obtain a system of equations whose general algebraic form is:

$$j_e - F_e \emptyset_p = A_E (\emptyset_P - \emptyset_E)$$

$$j_w - F_w \emptyset_p = A_W (\emptyset_W - \emptyset_P)$$

(III.15) $\qquad\qquad j_n - F_n \emptyset_p = A_N (\emptyset_P - \emptyset_N)$

$$j_s - F_s \emptyset_p = A_S (\emptyset_S - \emptyset_p)$$

$$A_P \emptyset_P = A_E \emptyset_E + A_W \emptyset_W + A_N \emptyset_N + A_S \emptyset_S + b$$

(III.16)

Or in equivalent form:

$$A_P \emptyset_P = \sum (A_{VS} \emptyset_{VS}) + b$$

$\emptyset$**:** is the variable in the equation concerned.

The indices (vs) represent the neighboring nodes of the main node.

The coefficients A_P and $\emptyset_{VS}$ are calculated with one of the methods with the problems of convection-diffusion (numerical scheme).

$$A_P = \sum A_{VS} + b \qquad \text{Or} \qquad A_P = A_E + A_W + A_N + A_S + \frac{\Delta X \Delta Y}{\Delta T}$$

A_P, A_E, A_W, A_N and A_S: corresponding coefficients, respectively, at the East, west, North, South and central control-volume nodes.

The general form of the discretized algebraic equation (III.16) where the total flow of convection and diffusion is calculated by a function **A (|P|) (Patankar 1980) (table2)**

$$A_E = D_e A(|P_e|) + max(-F_e, 0)$$

$$A_W = D_W A(|P_W|) + max(F_w, 0)$$

$$A_N = D_N A(|P_N|) + max(-F_n, 0)$$
(III.17)

$$A_S = D_S A(|P_S|) + max(F_s, 0)$$

$$b = (\overline{S_\emptyset} + \frac{\emptyset_P^T}{\Delta T})\Delta X \Delta Y$$

The coefficient of equation (III.16) contains a combination of the convective F and diffusion flux D at the control volume interfaces. The values of F and D and the peclet numbers for each interface, w, n and s of the control volume are given by the following relationships:

$$F_e = U_e \Delta Y \qquad\qquad F_w = U_w \Delta Y$$

$$F_n = U_n \Delta X \qquad\qquad F_s = U_s \Delta X$$

And
(III.18)

$$D_e = \frac{\Gamma_e}{dX_e}\Delta Y$$

$$D_w = \frac{\Gamma_w}{dX_w}\Delta Y$$

$$D_n = \frac{\Gamma_n}{dX_n}\Delta X$$

$$D_s = \frac{\Gamma_s}{dX_s}\Delta X$$

$$P_e = \frac{F_e}{D_e} \quad , \quad P_w = \frac{F_w}{D_w} \quad , \quad P_n = \frac{F_n}{D_n} \quad , \quad P_s = \frac{F_s}{D_s}$$
(III.19)

$A(|P_{ei}|)$ **:** is a function that characterizes the numerical interpolation scheme, which we will discuss in detail in the following.

III.3.2 function $A(|P|)$ for different numerical schemes

Expressions of the function $A(|P|)$ for different numerical schemes

Table (III.2): function $A(|P|)$ for different numerical schemes.

Scheme	Formula of the function $A(|P|)$
Different centers	$1 - 0.5|P|$
Upwind	1
Hybrid	$max[0.1 - 0.5|P|]$
Power law	$max[(0.1 - 0.5|P|)^5]$
Exponential	$|P|/[exp(|P|) - 1]$

In this work we use the Power Law scheme (Patankar 1980), as it requires less computing time and provides better stability of the numerical solution and results close to the exact solution.

III.4 Discretization of motion equation

(Patankar 1980), show that the integration of movement equations on the main control volume, leads to oscillatory solutions that have no physical meaning. To remedy this, he proposes a shift of the mesh for the velocity components. The discretization of the equations is obtained in the same way as the general transport equation. Only the geometric parameters change.

III.4.1 motion equation in the direction (ox)

Integrating the moment equation in the (ox) direction on control volumes shifted to the right, (see figure III.2), gives the algebraic equation:

$$\int_t^{t+\Delta t} \int_{s_v}^{n_v} \int_{w_u}^{e_u} \left[\frac{\partial U}{\partial T} + U\frac{\partial U}{\partial X} + V\frac{\partial U}{\partial Y}\right] dXdYdT = \int_t^{t+\Delta t} \int_{s_v}^{n_v} \int_{w_u}^{e_u} \left[-\frac{\partial P}{\partial X} + \frac{\mu_{nf}}{\rho_{nf}\alpha_f}\left(\frac{\partial^2 U}{\partial X^2} + \frac{\partial^2 U}{\partial Y^2}\right) + \right.$$

$$\left. \frac{(\rho\beta)_{nf}}{\rho_{nf}\beta_f}(R_a P_r \theta \cos(\alpha))\right] dXdYdT$$

(III.20)

We integrate term by term:

$$\int_t^{t+\Delta t} \int_{sv}^{n_v} \int_{w_u}^{e_u} \left[\frac{\partial U}{\partial T}\right] dXdYd\,T = \left(U_{pu}^{t+\Delta t} - U_{pu}^t\right)\Delta Y_P dX_e$$

(III.21)

$$\int_t^{t+\Delta t} \int_{S_v}^{n_v} \int_{w_u}^{e_u} \left[U \frac{\partial U}{\partial X} \right] dX dY d T = \int_t^{t+\Delta t} \int_{S_v}^{n_v} (U_{eu} U_{eu}^{t+\Delta t} - U_{eu} U_{eu}^{t+\Delta T}) dY dT = [U_{eu} \left(\frac{U_{Eu}^{t+\Delta t}+U_{Pu}^{t+\Delta t}}{2} \right) -$$

$$U_{wu} \left(\frac{U_{Pu}^{t+\Delta t}+U_{Wu}^{t+\Delta t}}{2} \right)] \Delta Y_P \Delta T$$

(III.22)

$$\int_t^{t+\Delta t} \int_{S_v}^{n_v} \int_{w_u}^{e_u} \left[V \frac{\partial U}{\partial X} \right] dX dY d T = \left[V_{nu} \left(\frac{U_{Pu}^{t+\Delta t}+U_{Nu}^{t+\Delta t}}{2} \right) - V_{su} \left(\frac{U_{Pu}^{t+\Delta t}+U_{Su}^{t+\Delta t}}{2} \right) \right] \Delta Y_P \Delta T$$

$$\int_t^{t+\Delta t} \int_{S_v}^{n_v} \int_{w_u}^{e_u} \left[-\frac{\partial P}{\partial X} \right] dX dY d T = (P_P^{t+\Delta t} - P_E^{t+\Delta t}) \Delta Y_P \Delta T$$

(III.23)

$$\int_t^{t+\Delta t} \int_{S_v}^{n_v} \int_{w_u}^{e_u} \left[\frac{\partial}{\partial X} \left(\frac{\partial U}{\partial X} \right) \right] dX dY dT = [\left(\frac{U_{Eu}^{t+\Delta t}-U_{Pu}^{t+\Delta t}}{dX_e} \right) - \left(\frac{U_{Pu}^{t+\Delta t}+U_{Wu}^{t+\Delta t}}{dX_p} \right)] \frac{\mu_{nf}}{\rho_{nf}\alpha_f} (\Delta Y_P \Delta T)$$

(III.24)

$$\int_t^{t+\Delta t} \int_{S_v}^{n_v} \int_{w_u}^{e_u} \left[\frac{\partial}{\partial Y} \left(\frac{\partial U}{\partial Y} \right) \right] dX dY dT = \left[\left(\frac{U_{Nu}^{t+\Delta t}-U_{Pu}^{t+\Delta t}}{dX_e} \right) - \left(\frac{U_{Pu}^{t+\Delta t}+U_{Su}^{t+\Delta t}}{dX_p} \right) \right] \frac{\mu_{nf}}{\rho_{nf}\alpha_f} (dX_e \Delta T)$$

(III.25)

Equation (III.20) will then be written:

$$\left[\frac{U_{eu}\Delta Y_P}{2} - \frac{U_{wu}\Delta Y_P}{2} + \frac{V_{nu}\Delta X_e}{2} - \frac{V_{su}\Delta X_e}{2} + \frac{\mu_{nf}}{\rho_{nf}\alpha_f} \frac{\Delta Y_P}{dX_e} + \frac{\mu_{nf}}{\rho_{nf}\alpha_f} \frac{\Delta Y_P}{dX_p} + \frac{\mu_{nf}}{\rho_{nf}\alpha_f} \frac{dX_e}{dY_n} + \frac{\mu_{nf}}{\rho_{nf}\alpha_f} \frac{dX_e}{dY_s} \frac{dX_e \Delta Y_P}{\Delta T} \right] U_P^{t+\Delta t} =$$

$$\left[-\frac{U_{eu}\Delta Y_P}{2} + \frac{\mu_{nf}}{\rho_{nf}\alpha_f} \frac{\Delta Y_P}{dX_e} \right] U_{Eu}^{t+\Delta t} + \left[\frac{U_{wu}\Delta Y_P}{2} + \frac{\mu_{nf}}{\rho_{nf}\alpha_f} \frac{\Delta Y_P}{dX_e} \right] U_{Wu}^{t+\Delta t} \left[-\frac{V_{nu}dX_e}{2} + \frac{\mu_{nf}}{\rho_{nf}\alpha_f} \frac{dX_e}{dY_n} \right] U_{Nn}^{t+\Delta t} +$$

$$\left[\frac{V_{su}dX_e}{2} + \frac{\mu_{nf}}{\rho_{nf}\alpha_f} \frac{dX_e}{dY_s} \right] U_{Su}^{t+\Delta t} + \left(P_P^{t+\Delta t} - P_E^{t+\Delta t} \right) \Delta Y_P + U_{pu}^t$$

(III.26)

In order to completely establish the discretize form of the following momentum equation (OX), integrating the continuity equation on the control volume shifted to the right and to the product of the equation by $U_{Pu}^{t+\Delta t}$ we will have:

$$\int_t^{t+\Delta t} \int_{sv}^{n_v} \int_{w_u}^{e_u} \left[\frac{\partial U}{\partial X} \right] dX dY d T + \int_t^{t+\Delta t} \int_{sv}^{n_v} \int_{w_u}^{e_u} \left[\frac{\partial V}{\partial Y} \right] dX dY d T = 0$$

(III.27)

We obtain:

$$[(U_{eu} - U_{wu})\Delta Y_P + (U_{nu} - U_{su})dX_e] U_{Pu}^{t+\Delta t} = 0$$

(III.28)

Then write the equation (III.26):

$$A_P U_{Pu}^{t+\Delta t} = A_E U_{Eu}^{t+\Delta t} + A_W U_{Wu}^{t+\Delta t} + A_N U_{Nu}^{t+\Delta t} + A_S U_{Su}^{t+\Delta t} + b$$

(III.29)

$$A_P = A_E + A_W + A_N + A_S + \frac{dX_e \Delta Y_p}{\Delta T}$$

$$b = \left(P_W^{t+\Delta t} - P_E^{t+\Delta t}\right)\Delta Y_P + \frac{dX_e \Delta Y_p}{\Delta T} U_{Pu}^T + R_a . P_r [\theta_W + \theta_E] . \sin(\alpha)\, \Delta Y_P dX_e$$

The coefficients A_i are already defined by the equations (III.16). the diffusive and convective flows are given by:

$$D_e = P_r \frac{\Delta Y_P}{dX_e} \quad F_e = U_{eu}\Delta Y_P$$

$$D_w = P_r \frac{\Delta Y_P}{dX_w} \quad F_w = U_{wu}\Delta Y_P$$

$$D_n = P_r \frac{dX_e}{dY_n} \quad F_n = V_{nu}dX_e$$

(III.30)

$$D_s = P_r \frac{dX_e}{dY_s} \quad F_s = V_{su}dX_e$$

With:

$$A_E = D_e A(|P_e|) + max(-F_e, 0)$$

$$A_W = D_W A(|P_W|) + max(F_w, 0)$$

$$A_N = D_N A(|P_N|) + max(-F_n, 0)$$

$$A_S = D_S A(|P_S|) + max(F_s, 0)$$

II.4.2 Motion equation in the direction (oy)

The integration of the momentum equation in the (oy) direction on the control volumes shifted upwards (see Figure 3).

Discretized this equation in the same equation of momentum equation following (ox), gives the following algebraic equation

$$A_P V_{PV}^{t+\Delta t} = A_E V_{EV}^{t+\Delta t} + A_W V_{WV}^{t+\Delta t} + A_N V_{NV}^{t+\Delta t} + A_S V_{SV}^{t+\Delta t} + b \qquad \text{(III.31)}$$

So:

$$A_P = A_E + A_W + A_N + A_S + \frac{\Delta X_P \Delta Y_n}{\Delta T}$$

$$b = \left(P_P^{t+\Delta t} - P_N^{t+\Delta t}\right)\Delta X_P + \frac{\Delta X_P dY_n}{\Delta T}V_{Pu}^T + R_a. P_r[\theta_P + \theta_N].\cos(\alpha)\,\Delta X_P dY_n$$

The diffusive and convective flows are given by :

$$D_e = P_r \frac{dY_n}{dX_e} F_e = U_{ev}dY_n$$

$$D_w = P_r \frac{dY_n}{dX_w} F_w = U_{wv}dY_n$$

$$D_n = P_r \frac{\Delta X_P}{dY_n} F_n = V_{nv}\Delta X_P$$

(III.32)

$$D_s = P_r \frac{\Delta X_P}{dY_s} F_s = V_{sv}\Delta X_P$$

With:

$$A_E = D_e A(|P_e|) + max(-F_e, 0)$$

$$A_W = D_W A(|P_W|) + max(F_w, 0)$$

$$A_N = D_N A(|P_N|) + max(-F_n, 0)$$

$$A_S = D_S A(|P_S|) + max(F_s, 0)$$

III.5 discretization of the energy equation

The integration of the energy equation on the typical control volumes corresponding to the nodes, see (figure III.1). Following the same steps of discretization of the general transport equation, gives the following algebraic equation:

$$A_P \theta_{PV}^{t+\Delta t} = A_E \theta_{E_V}^{t+\Delta t} + A_W \theta_{W_V}^{t+\Delta t} + A_N \theta_{N_V}^{t+\Delta t} + A_S \theta_{S_V}^{t+\Delta t} + b$$

(III.33)

So:

$$A_P = A_E + A_W + A_N + A_S + \frac{\Delta X \Delta Y}{\Delta T}$$

$$b = \frac{\Delta X. \Delta Y}{\Delta T}\theta_p^t$$

The diffusive and convective flows are given by:

$$D_e = \frac{\Delta Y}{dX_e} \quad F_e = U_e \Delta Y$$

$$D_w = \frac{\Delta Y}{dX_w} \quad F_w = U_w \Delta Y$$

(III.34)

$$D_n = \frac{\Delta X}{dX_n} \quad F_n = V_n \Delta X$$

$$D_s = \frac{\Delta X}{dX_s} \quad F_s = V_s \Delta X$$

With:

$$A_E = D_e A(|P_e|) + max(-F_e, 0)$$

$$A_W = D_W A(|P_W|) + max(F_w, 0)$$

$$A_N = D_N A(|P_N|) + max(-F_n, 0)$$

$$A_S = D_S A(|P_S|) + max(F_s, 0)$$

III.6   Algorithm solution for pressure-velocity coupling:

Algorithm solution for pressure-velocity coupling in steady flows is the standard prepossessing methods used to solve steady problems.

The advection of the scalar & used to define flow depends on the magnitude and direction of the local velocity field. In general, however the velocity field is not known. These algorithms are hence employed to obtain the solution.

And this Algorithm is:

III.6.1 the SIMPLER Algorithm

The word SIMPLER is the abbreviation of the first letters of the words: "Semi-Implicit method for pressure linked equation revised". The source terms in the equations of momentum table (III.1) depend on the pressure gradients; this during the absence of an equation governing the evolution of the pressure field makes the direct resolution of these equations impossible. To remedy these problems, the pressure field can be determined indirectly from the continuity equation. When a correct pressure field is injected into the momentum equations, the resulting velocity field will satisfy the continuity equation. This indirect information on the pressure field contained in the

continuity equation is transformed into direct information by the SIMPLER solving algorithm.

The pressure equation:

When the pressure field is known, the velocity field is obtained directly by the resolution of the motion quality equations. In the opposite case (pressure field unknown), the establishment of a pressure equation is necessary. The momentum equations discretized along the X, Y directions are written in the form:

$$A_P U_{Pu}^{t+\Delta t} = A_E U_{Eu}^{t+\Delta t} + A_W U_{Wu}^{t+\Delta t} + A_N U_{Nu}^{t+\Delta t} + A_S U_{Su}^{t+\Delta t} + b$$

(III.35)

$$A_P V_{PV}^{t+\Delta t} = A_E V_{EV}^{t+\Delta t} + A_W V_{WV}^{t+\Delta t} + A_N V_{NV}^{t+\Delta t} + A_S V_{SV}^{t+\Delta t} + b$$

(III.36)

$\left(\left(P_P^{t+\Delta t} - P_E^{t+\Delta t} \right) \Delta Y_P \right)$ and $\left(\left(P_P^{t+\Delta t} - P_N^{t+\Delta t} \right) \Delta X_P \right)$ respectively the pressure forces applied to the faces of the control volume. Velocity nicknames are defined by the following expressions:

$\boldsymbol{b_u}$ and $\boldsymbol{b_v}$: source without pressure term.

$$n_b = E, W, N, S$$

$$\widehat{U_{Pu}^{t+\Delta t}} = \left(\sum A_{nb_u} U_{nb_u}^{t+\Delta t} + b_u \right) / A_p \quad , \quad \widehat{V_{Pv}^{t+\Delta t}} = \left(\sum A_{nb_v} V_{nb_v}^{t+\Delta t} + b_v \right) / A_p$$

(III.37)

So the equation (III.35) and (III.36) become:

$$U_{Pu}^{t+\Delta t} = \widehat{U_{Pu}^{t+\Delta t}} + d_U \left(P_P^{t+\Delta t} - P_E^{t+\Delta t} \right) \quad , \quad V_{Pv}^{t+\Delta t} = \widehat{V_{Pv}^{t+\Delta t}} + d_V \left(P_P^{t+\Delta t} - P_N^{t+\Delta t} \right)$$

(III.38)

So the equation (III.35) and (III.36) become:

$$d_u = \Delta Y_p / A_p \qquad , \qquad d_v = \Delta X_p / A_p$$

(III.39)

The pressure equation can be obtained from the continuity equation by replacing the velocity expressions:

$$A_P P_P^{t+\Delta t} = A_E P_E^{t+\Delta t} + A_W P_W^{t+\Delta t} + A_N P_N^{t+\Delta t} + A_S P_S^{t+\Delta t} + S_p$$

(III.40)

$$A_E = d_U \Delta Y_P$$

$$A_W = d_U \Delta Y_P$$

$$A_N = d_V \Delta X_P$$

$$A_S = d_V \Delta X_P$$

$$A_P = A_E + A_W + A_N + A_S$$

$$S_P = \left(\widehat{U_{W_V}^{t+\Delta t}} - \widehat{U_{P_V}^{t+\Delta t}} \right) \Delta Y_P - \left(\widehat{U_{S_V}^{t+\Delta t}} - \widehat{U_{P_V}^{t+\Delta t}} \right) \Delta X_P$$

Pressure-correction equation:

For a guessed pressure field P*, we obtain the velocity field U*, V*, by the equations:

$$A_P U_{Pu^*}^{t+\Delta t} = \left(\sum A_{nb_u} U_{nb_u^*}^{t+\Delta t} + d_U \right) + (P_{P^*}^{t+\Delta t} - P_{E^*}^{t+\Delta t}) \Delta Y_P$$

(III.41)

$$A_P V_{Pv^*}^{t+\Delta t} = \left(\sum A_{nb_V} V_{nb_V^*}^{t+\Delta t} + d_V \right) + (P_{P^*}^{t+\Delta t} - P_{N^*}^{t+\Delta t}) \Delta X_P$$

(III.42)

A correct pressure field gives a correct velocity field satisfying the continuity equation. It is assumed that the correct values of pressure and velocity are obtained by the expressions:

$$P_P^{t+\Delta t} = P_{P^*}^{t+\Delta t} + {P'}_P^{t+\Delta t}$$

(III.43)

$$U_{Pu}^{t+\Delta t} = U_{Pu^*}^{t+\Delta t} + {U'}_{Pu}^{t+\Delta t}$$

(III.44)

$$V_{Pv}^{t+\Delta t} = V_{Pv^*}^{t+\Delta t} + {V'}_{Pv}^{t+\Delta t}$$

(III.45)

Where P'_P, U'_P, V'_P are respectively the pressure corrections field and the velocity field. These values must satisfy the momentum equations:

$$A_P \left(U_{Pu^*}^{t+\Delta t} + {U'}_{Pu}^{t+\Delta t} \right) = \left(\sum A_{nb_u} U_{nb_u^*}^{t+\Delta t} + d_U \right) + \left(P_{P^*}^{t+\Delta t} + {P'}_P^{t+\Delta t} - P_{E^*}^{t+\Delta t} + {P'}_E^{t+\Delta t} \right) \Delta Y_P$$

(III.46)

$$A_P \left(V_{Pv^*}^{t+\Delta t} + {V'}_{Pv}^{t+\Delta t} \right) = \left(\sum A_{nb_V} V_{nb_V^*}^{t+\Delta t} + d_V \right) + \left(P_{P^*}^{t+\Delta t} + {P'}_P^{t+\Delta t} - P_{N^*}^{t+\Delta t} + {P'}_N^{t+\Delta t} \right) \Delta X_P$$

(III.47)

Subtracting equations (III.40) from equations (III.41) we find:

46

$$A_P U'^{t+\Delta t}_{Pu} = \left(\sum A_{nb_u} U'^{t+\Delta t}_{nb_u} + d_U \right) + \left(P'^{t+\Delta t}_P - P'^{t+\Delta t}_E \right) \Delta Y_P$$

(III.48)

$$A_P V'^{t+\Delta t}_{Pv} = \left(\sum A_{nb_v} V'^{t+\Delta t}_{nb_v} + d_V \right) + \left(P'^{t+\Delta t}_P - P'^{t+\Delta t}_N \right) \Delta X_P$$

(III.49)

By making an approximation by eliminating summation terms, we obtain:

$$A_P U'^{t+\Delta t}_{Pu} = \left(P'^{t+\Delta t}_P - P'^{t+\Delta t}_E \right) \Delta Y_P$$

(III.50)

$$A_P V'^{t+\Delta t}_{Pv} = \left(P'^{t+\Delta t}_P - P'^{t+\Delta t}_N \right) \Delta X_P$$

(III.51)

So the corrected velocities according to the corrected pressure are:

$$U'^{t+\Delta t}_{Pu} = d_u \left(P'^{t+\Delta t}_P - P'^{t+\Delta t}_E \right)$$

(III.52)

$$V'^{t+\Delta t}_{Pv} = d_v \left(P'^{t+\Delta t}_P - P'^{t+\Delta t}_N \right)$$

(III.53)

So the expressions of equations (III.41) and (III.42) representing the correct values of pressure and velocity become:

$$P^{t+\Delta t}_P = \left(P^{t+\Delta t}_{P^*} - P'^{t+\Delta t}_P \right)$$

(III.54)

$$U^{t+\Delta t}_{P_u} = U^{t+\Delta t}_{P^*_u} + d_U \left(P'^{t+\Delta t}_P - P'^{t+\Delta t}_E \right)$$

(III.55)

$$V^{t+\Delta t}_{P_v} = V^{t+\Delta t}_{P^*_v} + d_V \left(P'^{t+\Delta t}_P - P'^{t+\Delta t}_N \right)$$

(III.56)

To arrive at the discretized pressure correction equation, the velocity expressions are replaced in the discretized continuity equation. We obtain:

$$A_P P'^{t+\Delta t}_P = A_E P'^{t+\Delta t}_E + A_W P'^{t+\Delta t}_W + A_N P'^{t+\Delta t}_N + A_S P'^{t+\Delta t}_S + S_{p'}$$

(III.57)

$$A_E = d_U . \Delta Y_P \quad , \quad A_W = d_u . \Delta Y_P \quad , \quad A_N = d_V . \Delta X_P \quad , \quad A_S = d_V . \Delta Y_P$$

$$A_P = A_E + A_W + A_N + A_S$$

$$S'_P = \left(U_{W_u^*}^{t+\Delta t} - U_{P_u^*}^{t+\Delta t}\right)\Delta Y_P + \left(V_{S_v^*}^{t+\Delta t} - V_{P_v^*}^{t+\Delta t}\right)\Delta X_P$$
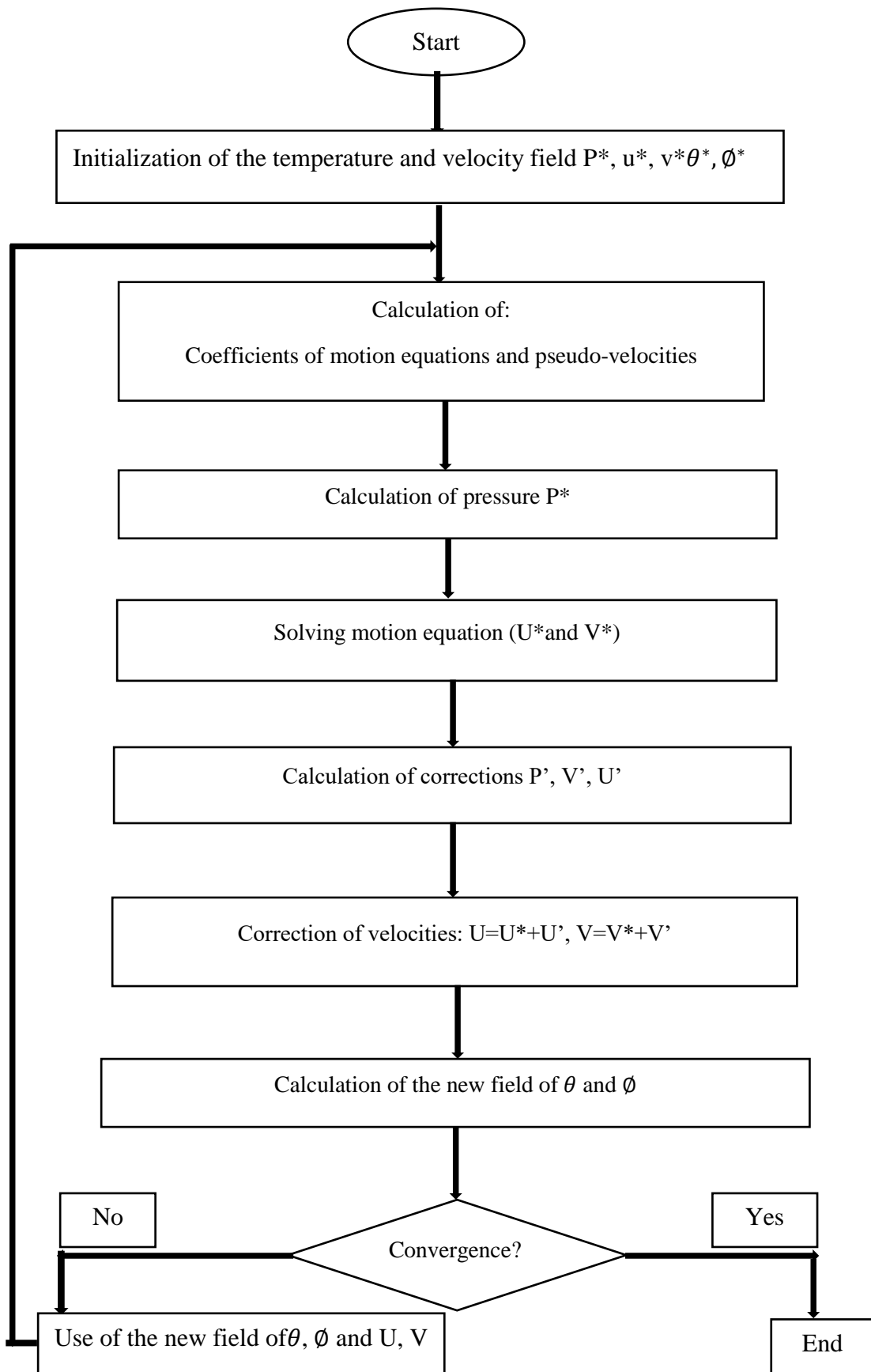
III.6.2 Sequences of the SIMPLER Algorithm

The revised algorithm consists of solving the pressure equation to obtain the pressure field and solving the pressure correction equation only to correct the velocities. The sequence of operations can be staled as:

1. Start with a guess velocity field.
2. Calculate the coefficients for the momentum equation and hence calculate $\widehat{U}$, $\widehat{V}$ from equations such as (III.35-36) by substituting values of the neighbor velocities $\boldsymbol{U_{nb}}$.
3. Calculate the coefficients for the pressure equation (III.40) and solve it to obtain the pressure field.
4. Treating this pressure field as P*, solve the momentum equations to obtain U*,V* from equation (III.41).
5. Calculate the mass source S_p from the pressure correction equation (III 56) and hence the P' equation.
6. Correct the velocity field by use of (III. 54.55.56)) but do not correct the pressure.
7. Solve the discretization equation for other(θ, φ).
8. Return to step 2 and repeat until convergence.

III.6.3 Motivation of the SIMPLER

The approximation introduced in deriving the P equation ((the omission of the term$\left(\sum A_{nb_u} U'^{t+\Delta t}_{nb_u}\right)$ leads to rather exaggerated pressure corrections, therefore under relaxation becomes necessary. Since the influence of the neighbor-point velocity corrections is eliminated from the velocity correction formula, the pressure correction has the whole burden of correcting the velocities, and this leads to a rather severe pressure-correction field. If the pressure- correction equation is only applied for the task of correcting the velocities and provide some other means of obtaining an improved pressure field, then a more efficient algorithm can be constructed. This is the essence of SIMPLER.

Start

Initialization of the temperature and velocity field P*, u*, v*θ*, $\emptyset$*

Calculation of:

Coefficients of motion equations and pseudo-velocities

Calculation of pressure P*

Solving motion equation (U*and V*)

Calculation of corrections P', V', U'

Correction of velocities: U=U*+U', V=V*+V'

Calculation of the new field of θ and $\emptyset$

No

Yes

Convergence?

Use of the new field of θ, $\emptyset$ and U, V

End

CHAPTER IV

RESULTS AND DESCENT

IV.1 Introduction

In this chapter, we focus on the numerical study of natural convection. We will first see the influence of the mesh on the results, and then we proceed to the validation of our calculation code by comparing our results with those obtained in the previous studies.

We present for natural convection the isotherms and the current lines, as well as the profiles of the temperature, and of the velocity we also present a study relative to the thermal transfer considering the local Nusselt number.

We use the following parameters: $500 \leq \mathrm{Ra} \leq 10^6$, $0 \leq \varphi \leq 0.2$, $\mathrm{Pr} = 6.2$, $0 \leq \alpha \leq 90$.

The nanofluids considered are: Cu-water, Al2o3-water and Au-water.

IV.2 Mesh choice

The structure and size of the grid can have a significant effect on the obtained results. For this reason, it is advisable to test the sensitivity of our results to the selected mesh sizes. **Table (IV.1)** and figure (IV.1) show the effect of the mesh size on the average Nusselt number. In order to obtain an accurate results and a good spatial resolution, the mesh (80*80) has been selected and used in all calculations.

Table (IV.1): The effect of mesh on the average Nusselt number.

Ra = 10^6 ; $\alpha = 0°$; $\varphi = 0.03$									
Mesh	20*20	30*30	40*40	50*50	60*60	70*70	80*80	90*90	100*100
$\overline{Nu}$ (Cu+water)	10.971	10.317	9.895	9.687	9.573	9.504	9.459	9.428	9.406
$\overline{Nu}$(AL2O3+Water)	10.882	10.230	9.813	9.609	9.496	9.428	9.384	9.384	9.384
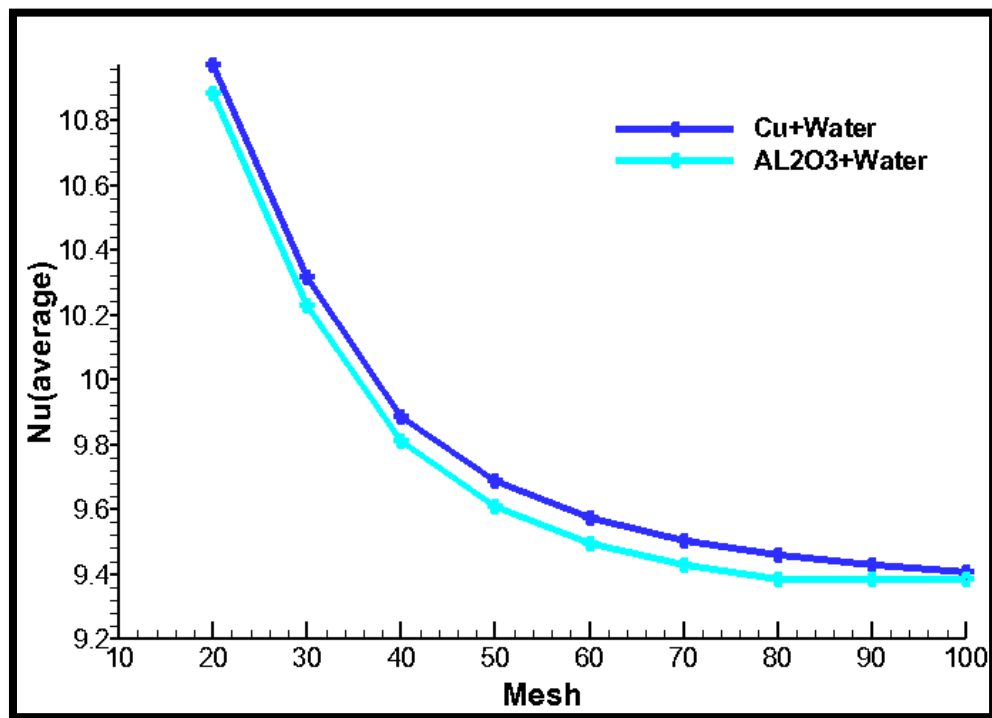
Figure (IV.1): Evolution of average heat transfer with the different meshes.

IV.3 Code validation

Before starting the numerical calculations, governing the dynamic and thermal flow, the validation of our model is based on a quantitative and qualitative comparison with other investigations available in the literature to give more credibility to the results of our numerical simulations. The present numerical solution is further validated by comparison the present code against the numerical simulation of Hakan F.Oztop Eiyad Abu-Nada [17] The first comparison was made for Pr= 0.70 and $10^3 \leq Ra \leq 10^6$. Figure (IV.2) shows the variation of the average Nusselt number with Raileigh number. A second comparison of streamlines (on the left) and isotherms (on the right) is shown in figure IV.3 for: Cu-water nanofluid, Ra= 10^5 and volume fraction φ =0.1 and 0.2. A good agreement between the two works is observed.
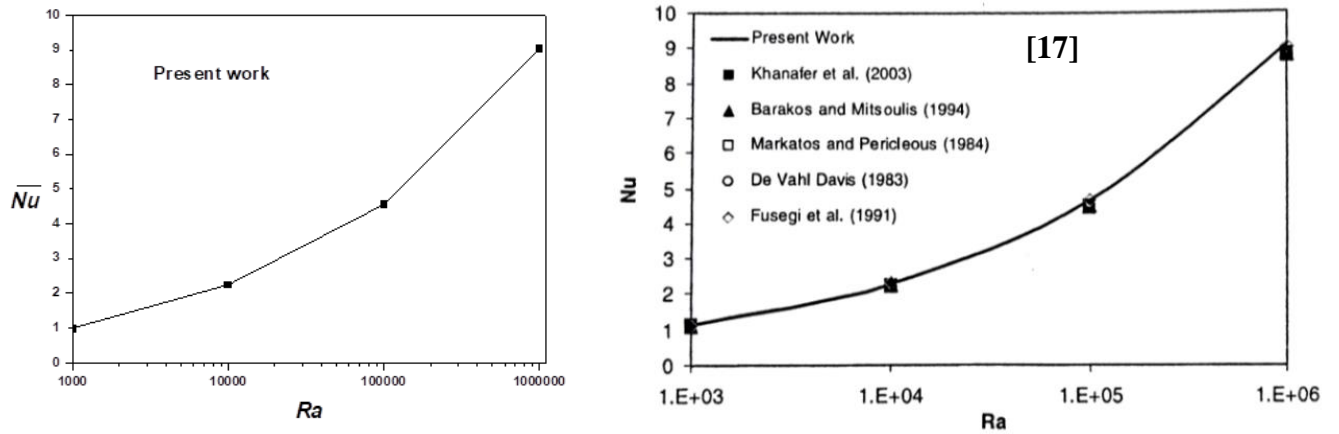
Figure (IV.2): Nusselt number versus Rayleigh number and comparison with other published works.
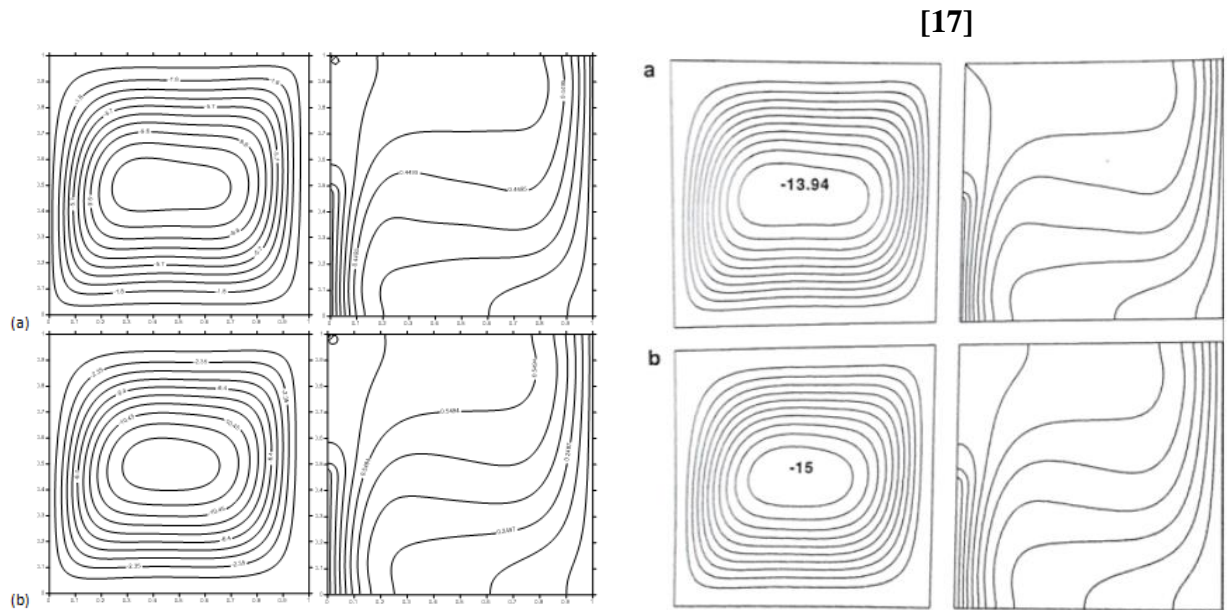
Figure (IV.3): Streamlines and isotherms for Cu-water, Ra=10^5, A=1. (a) $\varphi = 0.1$, (b) $\varphi = 0.2$.

IV.4 Effect of Rayleigh number

In order to examine the influence of Rayleigh number on physical phenomenon, we have executed the calculation program in the cases: pure fluid (water with **φ=0**) and Cu-water nanofluid (φ=0.03 and 0.2).

A.   Flow structure

Figure IV.4 indicates that the flow is formed with a single-cell which occupies the most of the cavity. By increasing the number of Rayleigh, the shape of this cell changes from circular to elliptic one for high Rayleigh number (Ra=10^6).

We notice that the current lines are symmetric in relation to the center of the cavity. The intensity of these lines decreases when we approach the center of the cavity.

$\varphi = 0$ $\varphi = 0.03$ (Cu+Water) $\varphi = 0.2$ (Cu+Water)

Ra $= 10^3$

Ra $= 10^4$

Ra $= 10^5$

Ra $= 10^6$
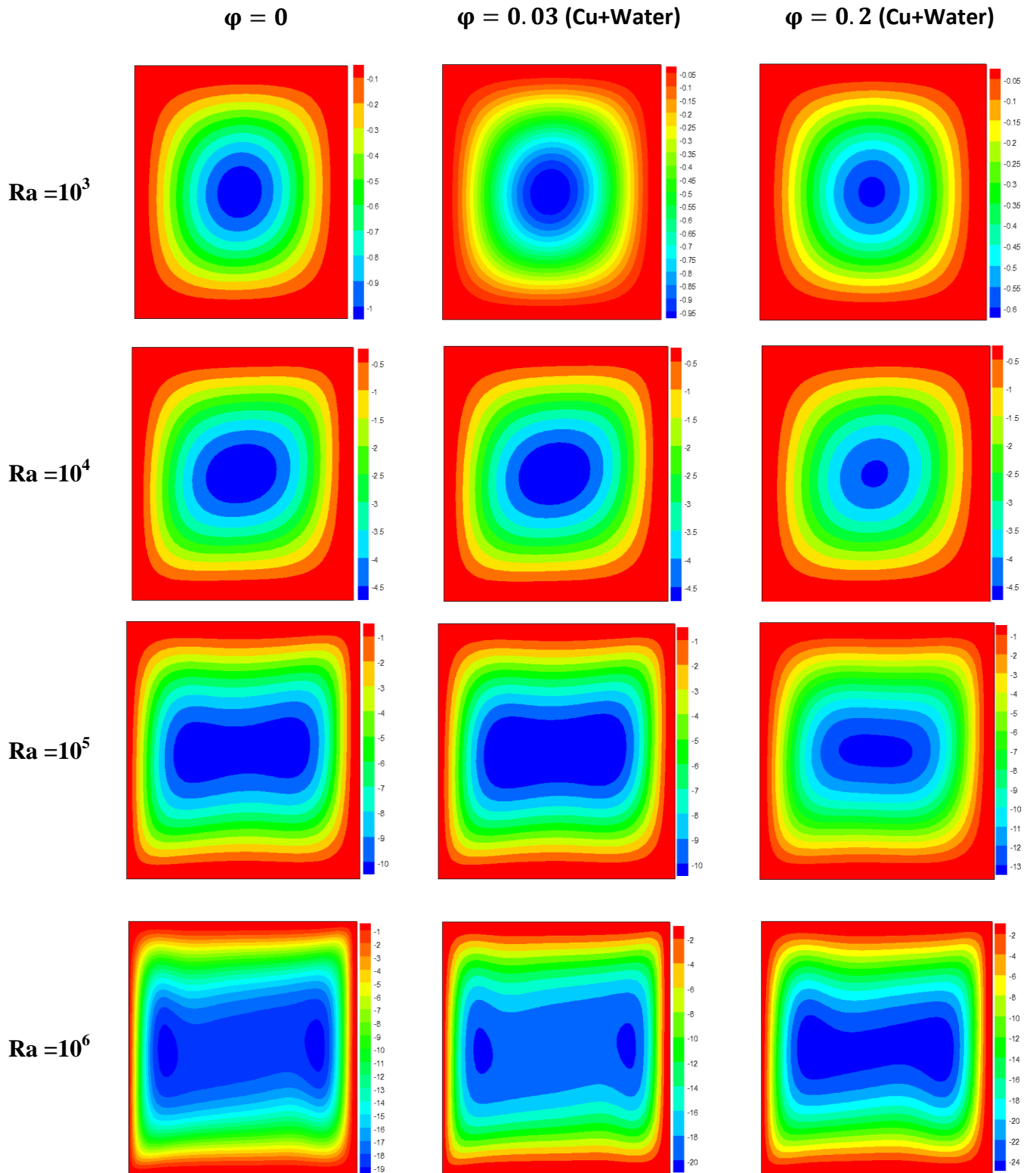
Figure (IV.4): Stream lines for different values of Rayleigh number.

Maximum velocity in the enclosure for different volume fraction increases with Rayleigh number as shown in figure IV.5.
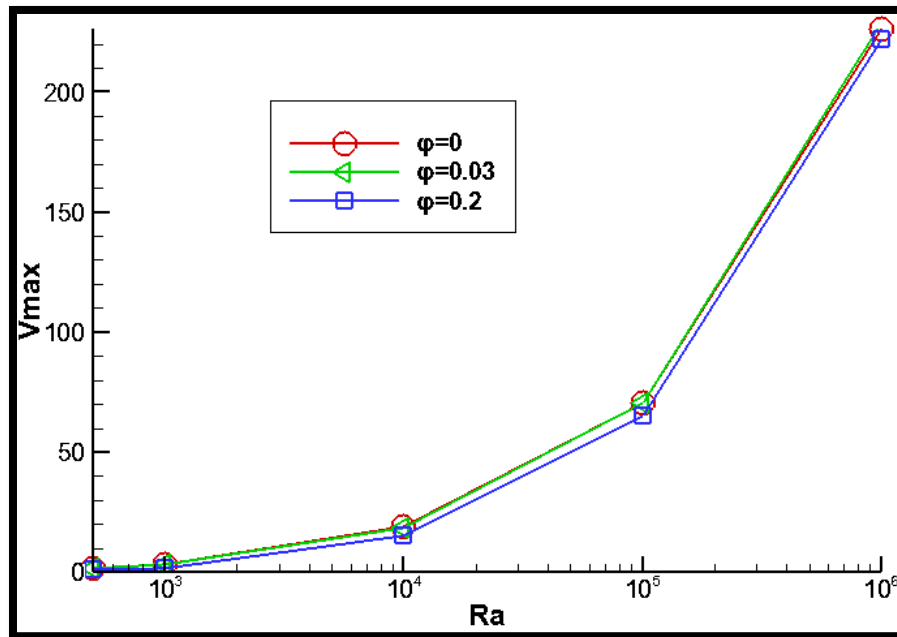
Figure (IV.5): Variation of maximum velocity with Rayleigh number.

B.   Heat Transfer Phenomena

Figure (IV.6) illustrates the distribution of temperature within the nanofluid for different values of Rayleigh number and volume fractions. When Ra=500 the isothermal lines are nearly parallel to the vertical walls. The heat transfer is therefore purely conductive. The temperature varies progressively from the left wall to the cold right wall. When Ra takes the value 10^4, the isothermal lines are deformed in the direction flow. This deformation is more and more important when Ra increases indicating the dominance of the convective regime of heat transfer. The isotherms are more concentrated near the vertical walls showing a strong temperature gradient in these regions. The same behavior can be observed in **figure (IV.7)** showing the evolution of the average Nusselt number on the hot wall as a function of the Rayleigh number for $\varphi = 0$ and 0.2. Heat transfer rate is thus an increasing function with Ra. We can also observe, on the same **figure (IV.7)**, that the presence of nanoparticles in the base fluid improves the thermal exchange because of the increase of thermal conductivity.
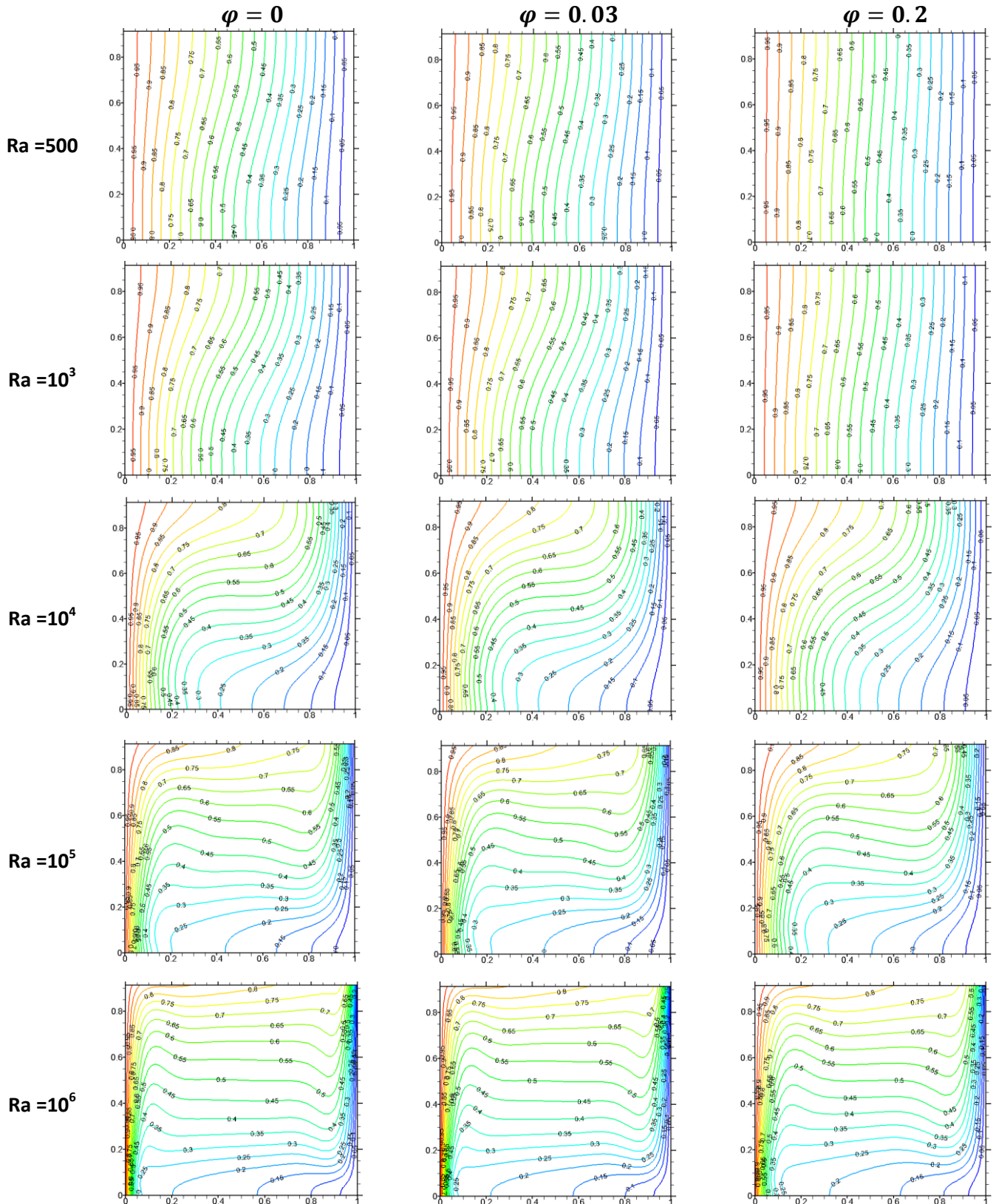
Figure (IV.6): isothermal lines for different values of Rayleigh number for Cu-water.

The increase of volume fractions results in an important deviation for the isothermals between the nanofluid and the pure fluid.

Generally, we distinguish three flow regimes according to the Rayleigh number. The Rayleigh numbers Ra $>10^5$ the convective regime corresponding to the convection (called boundary layer). The second flow regime is conductive. It is the dominant character for low Rayleigh numbers Ra $< 10^4$. The third regime is called transitory $10^4 \le Ra \le 10^5$. The two regimes convective and conductive are responsible for the transfer of the heat in the cavity.
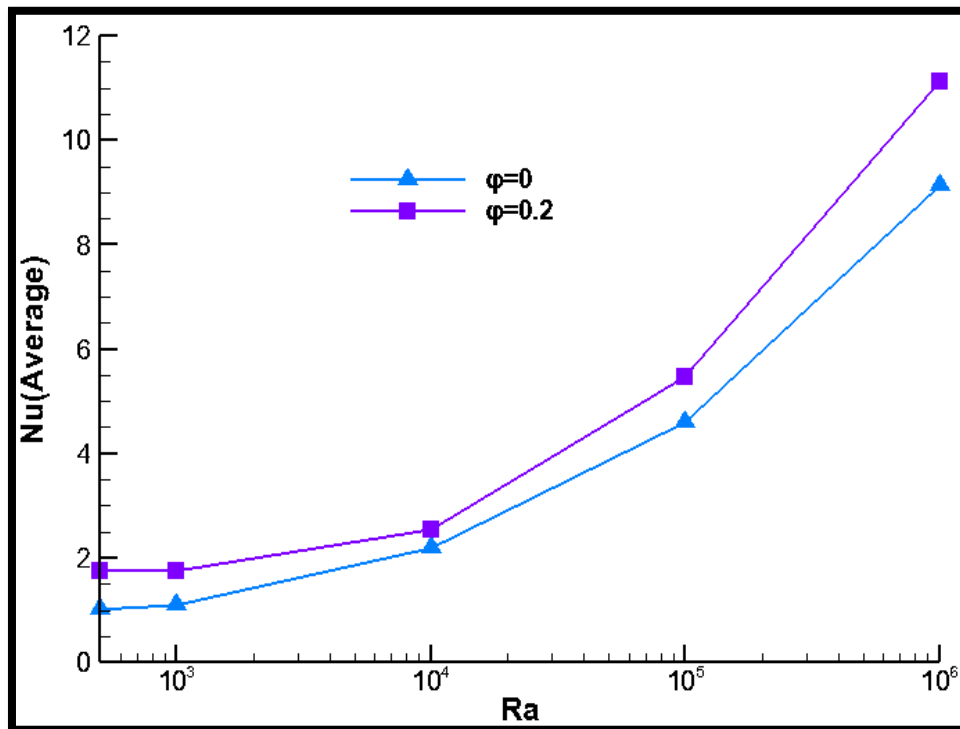
Figure (IV.7): Variation of the average Nusselt number as a function of Rayleigh number.

IV. 5 Effect of nanoparticle volume fraction

For Cu-water nano-fluid, figures (IV.8) and (IV.9) illustrate the evolution of respectively the average Nusselt number as a function of volume fraction for three values of Rayleigh number (500, 10^4 and 10^6) and the local Nusselt number with φ for Ra=10^6.

We notice that the increase of nanoparticle volume fraction increases heat transfer rate and local heat exchange whatever the value of Ra. The heat propagation is thus improved by the increase of the percentage of nanoparticles in the base fluid.
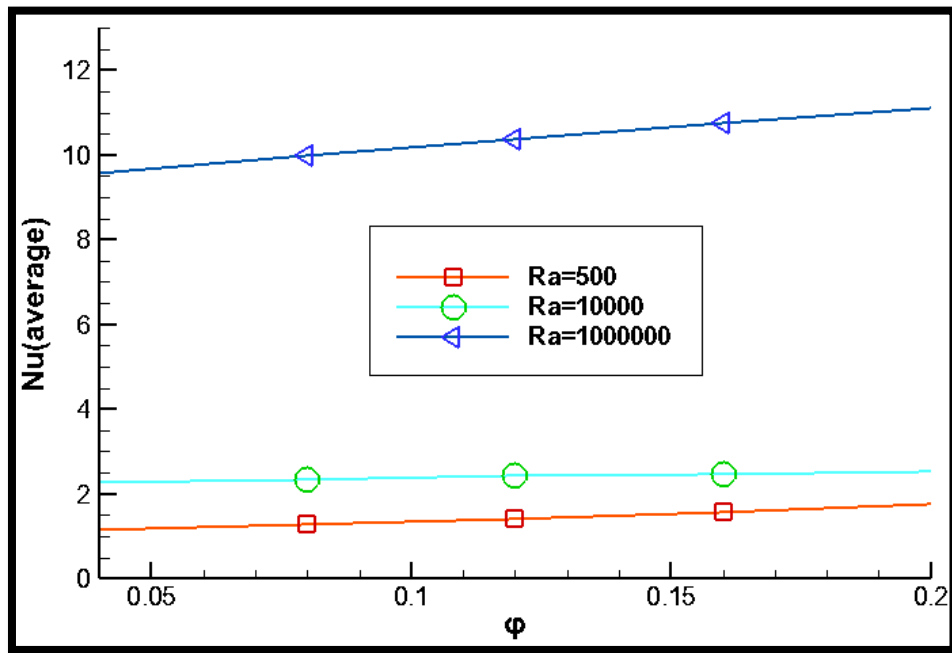
55

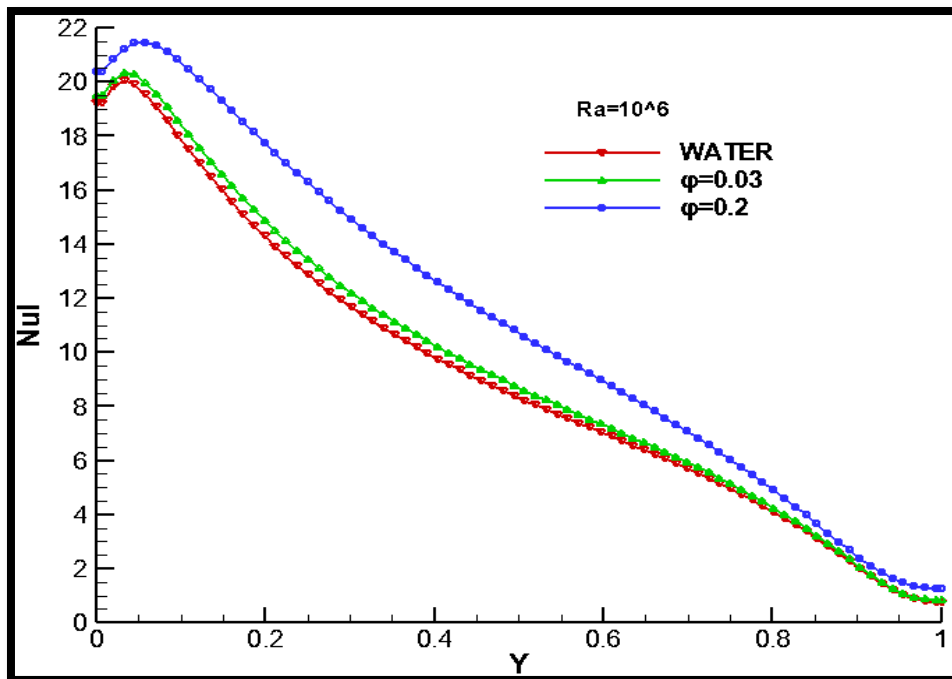**Figure (IV.8):** Variation of the average Nusselt number as a function of volume fraction.

Figure (IV.9): Variation of the local Nusselt number as a function of volume fraction with Ra=10^6.

IV.6 Effect of nanoparticle types

The effect of the nature of nanofluid on heat exchange by natural convection within the cavity is studied using different nanofluids with different concentrations: Cu-water, Au-water and AL2O3-water, figure (IV.10, 11 and 12).

Figure (IV.10): shows that the average Nusselt number on the hot wall increases linearly when increasing the concentration of nanoparticles. The minimum heat transfer rate is obtained for Au-water.

Figures (IV.11), (IV.12) and (IV.13): The temperature value increases with an increase in the concentration of nanoparticles, and the velocity decreases.
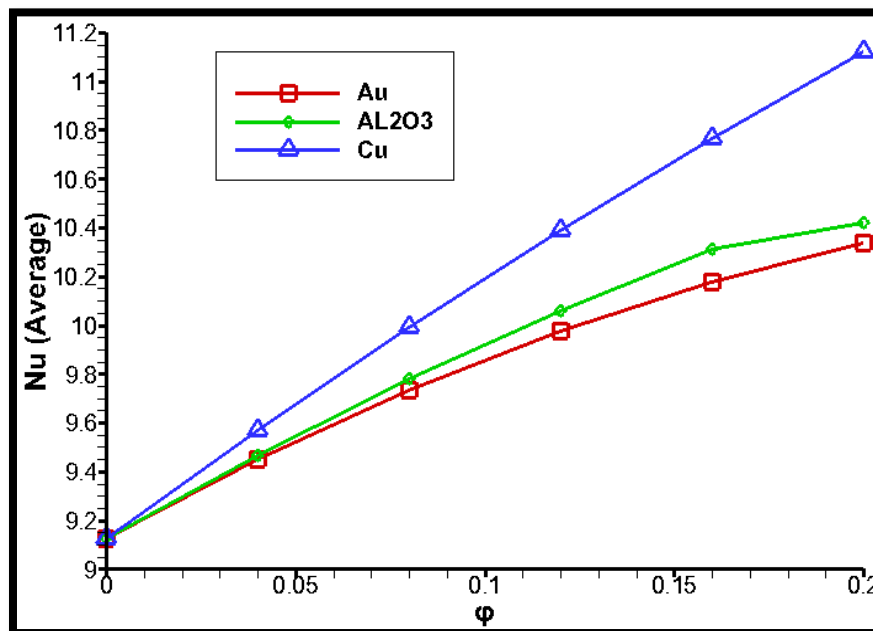
Figure (IV.10): Variation of the average Nusselt number as a function of volume fraction
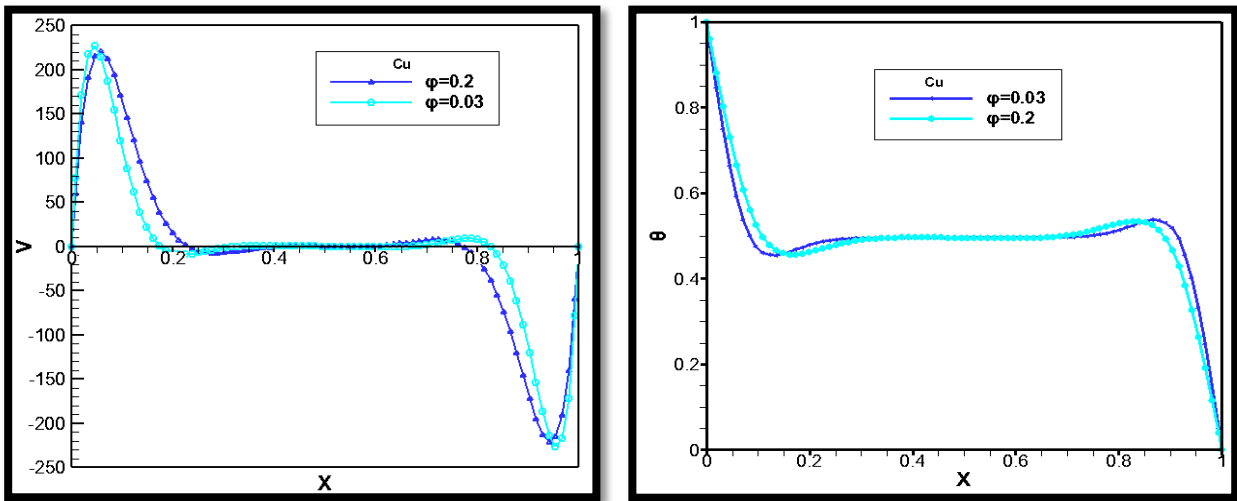
and the type of nanoparticles. Ra=10^6.

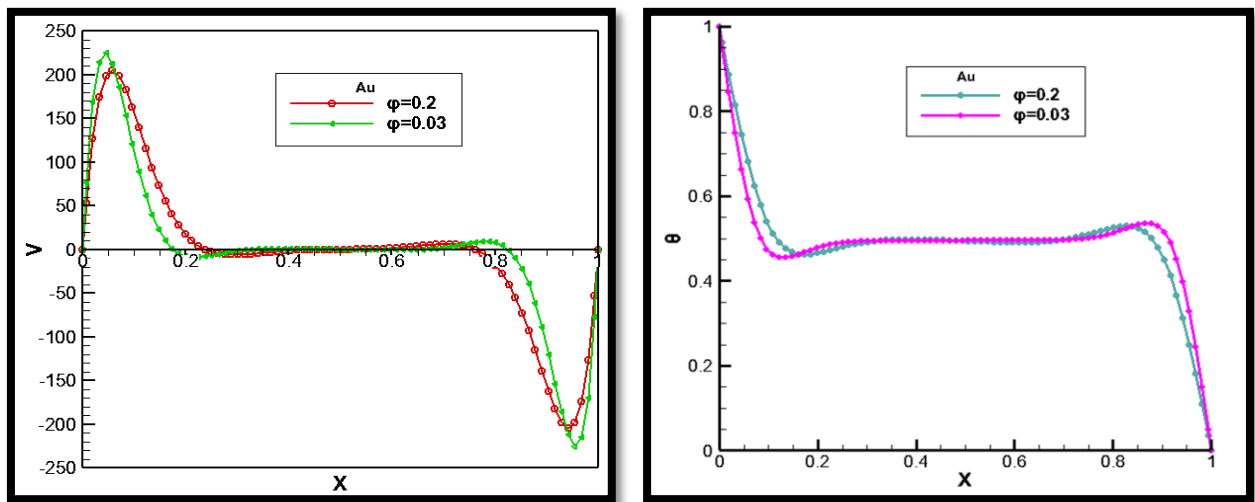**Figure (IV.11):** Velocity and temperature profiles at the middle of the enclosure for Cu Ra=10^6.

Figure (IV.12): Velocity and temperature profiles at the middle of the enclosure for Au Ra=10^6.
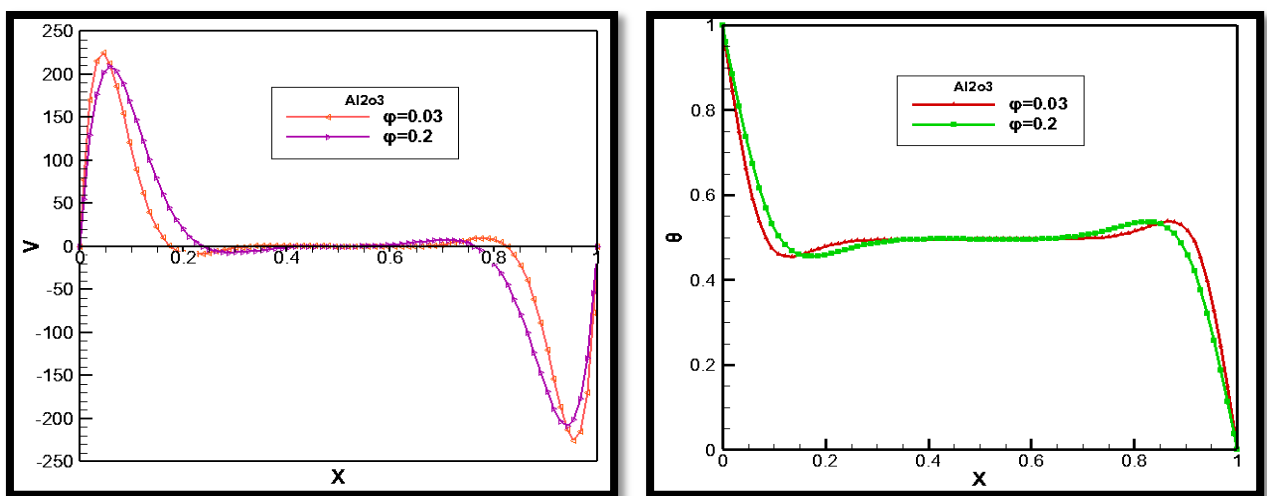

Figure (IV.13): Velocity and temperature profiles at the middle of the enclosure for Al2o3 Ra=10^6.

58

IV.7 Effect of inclination angle

For the analysis of the influence of inclination angle on fluid flow, the isothermals and current lines are presented in relation to each inclination angle, which varies between 0° and 90° **figure (IV.13)**. The flow is characterized by a monocellular centro symmetric structure for $\alpha < 90°$. It becomes bicellular for $\alpha = 90$.

The average Nusselt number depends on the inclination angle **figure (IV.14)**. The increase of α between 0° and 30°, accentuates heat transfer to reach a maximum value when $\alpha = 30°$. Beyond 30° the Nusselt number starts to decrease to reach its minimum value for an angle of 90°.

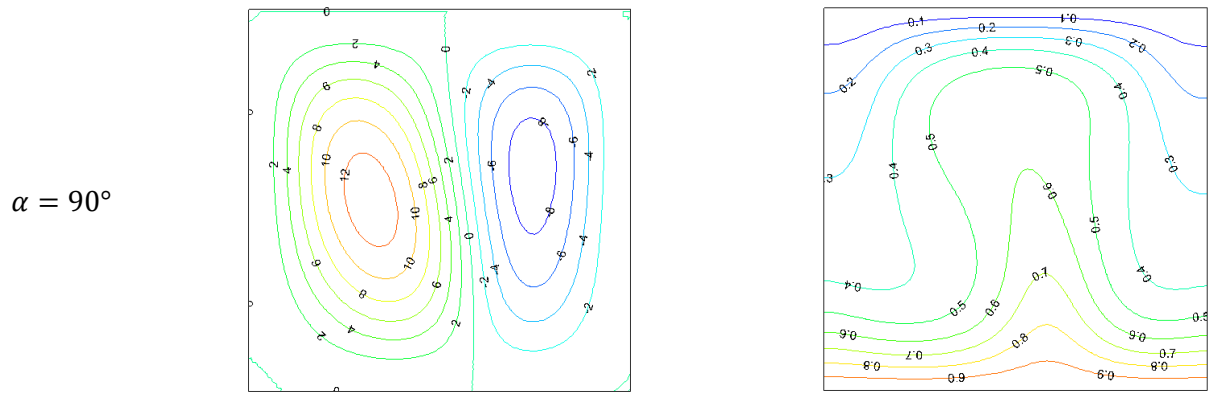Gravity prevents the transmission of heat and the speed of the nanofluid with different angle values between 0 and 90.

$\alpha = 0°$

$\alpha = 30°$

$\alpha = 45°$

$\alpha = 60°$

$\alpha = 75°$

$\alpha = 90°$
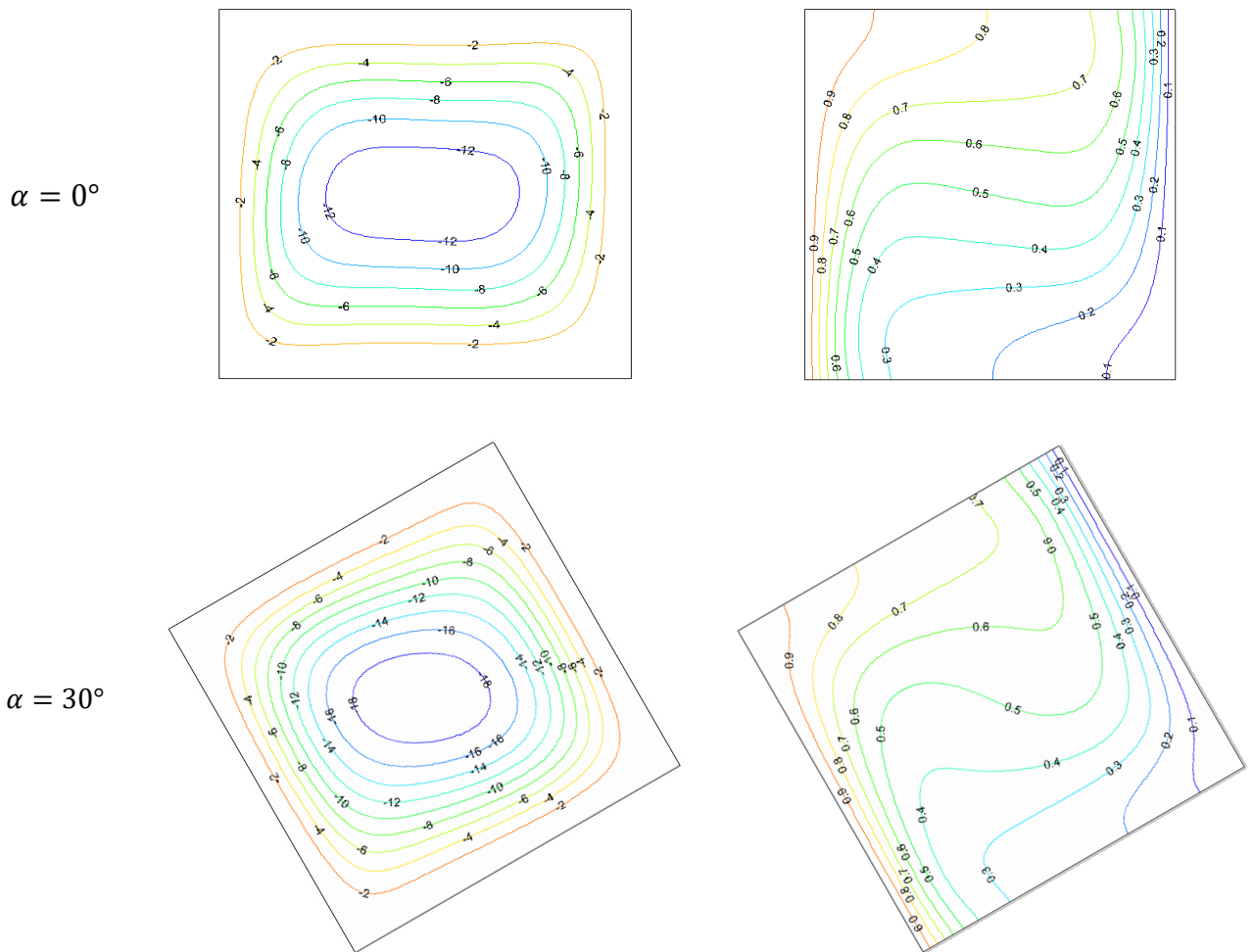
Figure (IV.14): Stream lines and isothermal lines for different values of inclination angle for
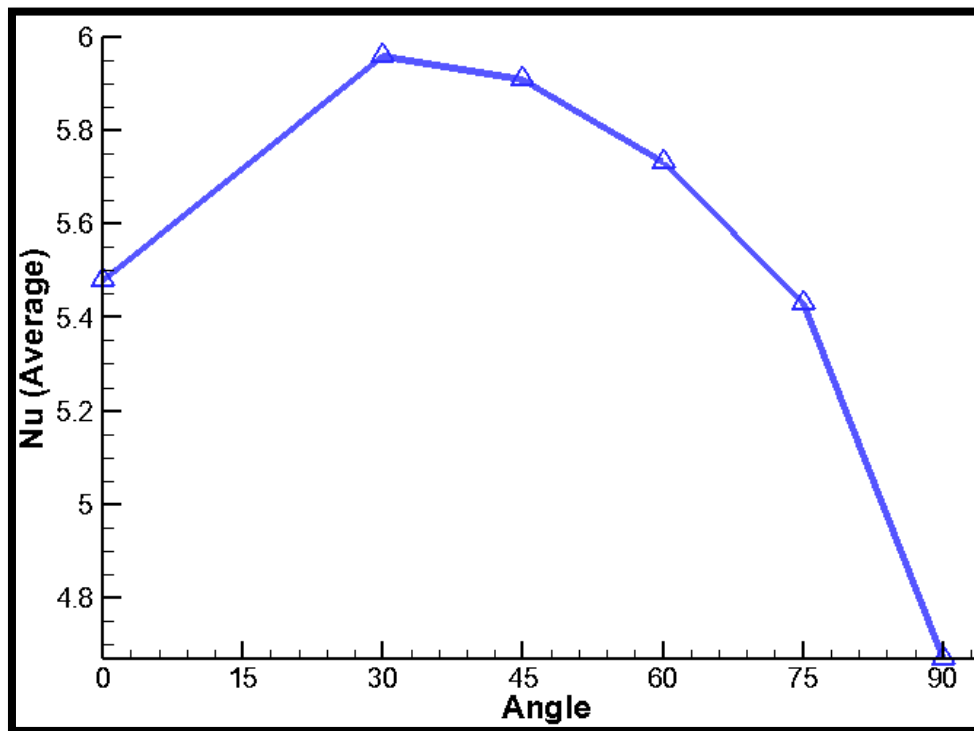
Cu-water, Ra=10^5, $\varphi = 0.2$.

Figure (IV.15): Variation of the average Nusselt number as a function of inclination angles for

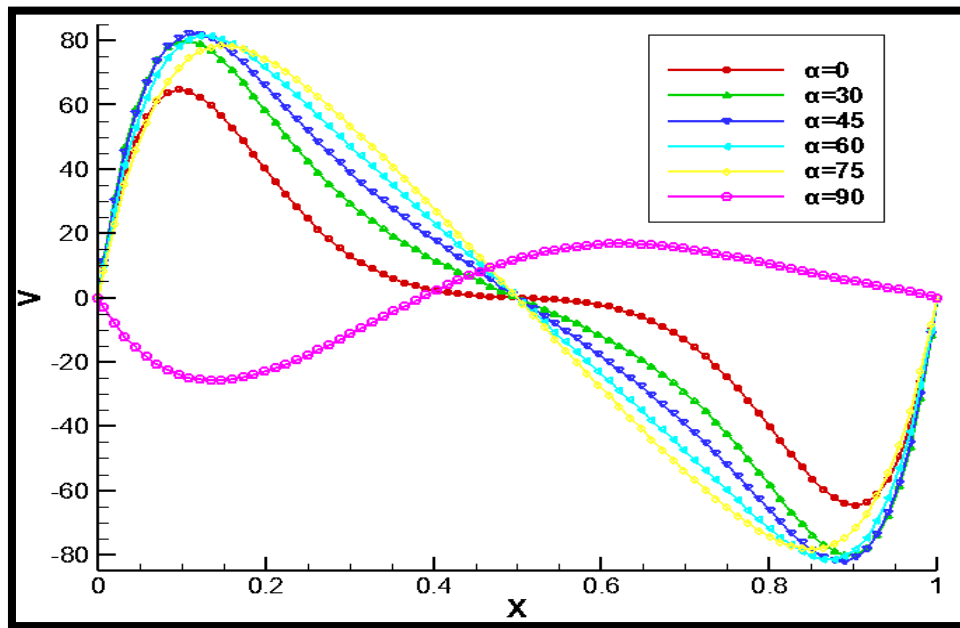Cu-water, Ra=10^5, $\varphi = 0.2$.

Figure (IV.16): Velocity profiles for different inclination angles.

IV.8 Conclusion

In this chapter, we have presented the different results showing the effect of Rayleigh number and the types of nanoparticles on heat transfer and velocity flow in the enclosure. The effect of inclination angle of the cavity and volume fraction of nanoparticles is also taken in consideration.

In general, three flow regimes can be distinguished according to the Rayleigh number. Convective regime corresponding to Ra $>10^5$ (called boundary layer). The second flow regime is conductive. This is the dominant character for low Rayleigh numbers Ra $< 10^4$. While for $10^4 \leq Ra \leq 10^5$, the third regime is called transient. Both convective and conductive regimes are responsible for heat transfer in the cavity.

Both increasing the value of Rayleigh number and volume fraction enhances heat transfer in the enclosure. The highest values of heat transfer are obtained when using Cu nanoparticles. For the same nanofluid and the same parameters, heat transfer reaches its maximum value when $\alpha=30°$. White it takes its minimum value for $\alpha=90°$.

GENERAL CONCLUSION

Conclusion

In this memory, we presented a numerical study on the natural convection of the nanofluid to see its effects on thermal transport, with a two-dimensional Cartesian geometry shape with a thermal source in the left vertical wall.

The governing equations have been solved by finite volume method and using the numerical simulation to obtain precise results of local and average Nusselt numbers, flow structure, and temperature field. The objective of the study is to show the effect of: the types and the volume fraction of nanoparticles in the base fluid (water).The effect of Rayleigh number and the inclination angle of the enclosure is also considered. We got the following results:

1- The presence of nanoparticles in a base fluid modifies the dynamic and thermal fields of the convective flow.

2- Increasing the value of the Rayleigh number improves the heat transfer and flow intensity.

3- The heat exchange in the enclosure increases with the increase in the volume fraction of the nanoparticles.

4- Metallic type nanoparticles (Cu) offer better heat propagation.

5- The variation of inclination angle changes the dynamic and thermal fields of the convective flow.

6- For the same nanofluid and the same parameters, heat transfer reaches its maximum value when $\varphi=30°$. White it takes its minimum value for $\varphi=90°$.

In the future, the study can be extended for higher Rayleigh numbers, different types of nanofluids and other geometries.

BIBLIOGRAPHIC

Bibliographic

[1] W. Yu, S.U.S. Choi. Le rôle des couches interfaciales dans la conductivité thermique améliorée des nanofluides : un modèle Maxwell rénové. , 5 (1-2), 167-171, (2003) .doi : 10.1023 / a : 1024438603801.

[2] E.E. (Stathis) Michaelides, Nanofluidics: Thermodynamic and Transport Properties, Springer International Publishing Switzerland. 2014.

[3] Okba, B, A. Développement thermique de l'écoulement d'un nano fluide entre deux plaques parallèles. Mémoire master : Mécanique Energétique. Université Mohamed Khider de Biskra: Faculté Des Sciences et de la Technologie Département de Génie Mécanique.36, (2021).

[4] https://www.intechopen.com/chapters/68881

[5] Kamel, C, Modélisation et simulation du refroidissement des éléments à base de composants électroniques par des nanofluides. Thèse doctorat en sciences : Mécanique énergétique. Université Mohamed khider_Biskra : faculté des sciences et de la technologie.163.

[6] Hanen, Fet Cherif, K. Etude numérique de la convection naturelle dans une cavité différentiellement chauffée remplie de nano-fluide. Mémoire de Master: Universite Mohamed boudiaf - Msila. (2020).

[7] Brinkman H.C., The Viscosity of Concentrated Suspensions and Solutions, J. Chemical Physics, Vol. 20, pp. 571, 1952.

[8] Soufi E. H., Application des nanofluides pour le refroidissement : Etude d'un cas d'une géométrie simple', Université Kasdi Merbah d'Ouargla, 2013.

[9] Routbort J., et al., Argonne National Lab, Michelin North America, St. Gobain Corp., 2009, http://www1.eere.energy .gov/industry/nanomanufacturing/pdfs/nanofluids industrial cooling.pdf.

[10] Han Z. H., Cao F. Y., and Yang B., Synthesis and thermal characterization of phase-changeable indium/polyalphaolefin nanofluids, Applied Physics letters, vol. 92, no. 24, Article ID 243104, 3 pages, 2008.

[11] Walid B. et Mohamed A. Etude de transfert de chaleur de nanofluide dans une cavité carrée sous champ magnétique. Master énergétique. Université de bouira : faculté des sciences et des sciences appliquées département de génie mécanique.70 (2020).

BIBLIOGRAPHIC

[12] https://www.unilab.eu/articles/technical-articles/thermodynamic-engineering-articles/nanofluids/#mobile-menu.

[13] Bouton M., Evaluation de l'intérêt énergétique des nanofluids dans l'usage des machines frigorifiques, 2012.

[14] Walid, B et Mohammed, A. Etude de transfert de chaleur de nanofluide dans une cavité carrée sous champ magnétique. Mémoire Master Recherche : Mécanique Energétique. Universite de Bouira : Faculté des Sciences et des Sciences Appliquées Département de Génie Mécanique, 53. (2020).

[15] S. V. Patankar and D. B. Spalding, A Calculation Procedure for Heat, Mass and Momentum transfer in three-dimensional Parabolic Flows, Int. J. Heat Mass Transfer, 15, 1787– 1790 (1972).

[16] E. Belahmadi, Simulation numérique de la convection naturelle dans une cavité carrée poreuse, Mémoire Magister en Génie mécanique, Université de Constantine 1, (2013)

[17] Hakan F.Oztop[a], Eiyad Abu-Nada[b]. Numerical study of natural convection in partially heated rectangular enclosures filled with nanofluids. International journal of Heat and fluid flow 29 (2008) 1326-1336.